

Molecular characterisation of the vacuolating autotransporter toxin in uropathogenic escherichia coli

Nichols, Katie B; Totsika, Makrina; Moriel, Danilo G; Lo, Alvin W; Yang, Ji; Wurpel, Daniël J; Rossiter, Amanda E; Strugnell, Richard A; Henderson, Ian R; Ulett, Glen C; Beatson, Scott A; Schembri, Mark A

DOI:
[10.1128/JB.00791-15](https://doi.org/10.1128/JB.00791-15)

License:
None: All rights reserved

Document Version
Peer reviewed version

Citation for published version (Harvard):
Nichols, KB, Totsika, M, Moriel, DG, Lo, AW, Yang, J, Wurpel, DJ, Rossiter, AE, Strugnell, RA, Henderson, IR, Ulett, GC, Beatson, SA & Schembri, MA 2016, 'Molecular characterisation of the vacuolating autotransporter toxin in uropathogenic escherichia coli', *Journal of Bacteriology*. <https://doi.org/10.1128/JB.00791-15>

[Link to publication on Research at Birmingham portal](#)

Publisher Rights Statement:
Checked for eligibility: 31/05/2016

General rights

Unless a licence is specified above, all rights (including copyright and moral rights) in this document are retained by the authors and/or the copyright holders. The express permission of the copyright holder must be obtained for any use of this material other than for purposes permitted by law.

- Users may freely distribute the URL that is used to identify this publication.
- Users may download and/or print one copy of the publication from the University of Birmingham research portal for the purpose of private study or non-commercial research.
- User may use extracts from the document in line with the concept of 'fair dealing' under the Copyright, Designs and Patents Act 1988 (?)
- Users may not further distribute the material nor use it for the purposes of commercial gain.

Where a licence is displayed above, please note the terms and conditions of the licence govern your use of this document.

When citing, please reference the published version.

Take down policy

While the University of Birmingham exercises care and attention in making items available there are rare occasions when an item has been uploaded in error or has been deemed to be commercially or otherwise sensitive.

If you believe that this is the case for this document, please contact UBIRA@lists.bham.ac.uk providing details and we will remove access to the work immediately and investigate.

1 **Molecular characterisation of the Vacuolating Autotransporter**
2 **Toxin in Uropathogenic *Escherichia coli***

3 Katie B. Nichols¹, Makrina Totsika², Danilo G. Moriel¹, Alvin W. Lo¹, Ji Yang³, Daniël J.
4 Wurpel¹, Amanda E. Rossiter³, Richard A. Strugnell³, Ian R. Henderson⁴, Glen C. Ulett⁵, Scott
5 A. Beatson¹ and Mark A. Schembri^{1*}

6
7 ¹*Australian Infectious Disease Research Centre, School of Chemistry and Molecular*
8 *Biosciences, University of Queensland, Brisbane, Queensland, Australia.*

9 ²*Institute of Health and Biomedical Innovation, School of Biomedical Sciences, Queensland*
10 *University of Technology, Brisbane, Queensland, Australia*

11 ³*Department of Microbiology and Immunology, The University of Melbourne at the Peter*
12 *Doherty Institute for Infection and Immunity, Melbourne, Australia*

13 ⁴*Institute of Microbiology and Infection, School of Immunity and Infection, University of*
14 *Birmingham, Birmingham, B15 2TT, United Kingdom*

15 ⁵*School of Medical Science, Menzies Health Institute Queensland, Griffith University, Gold*
16 *Coast, Queensland, Australia*

17
18 Running title: Characterisation of Vat in UPEC

19
20 Key words: Uropathogenic *Escherichia coli*, urinary tract infection, autotransporter, serine
21 protease, vacuolating autotransporter toxin.

22
23
24 * **Corresponding author.**

25 Mailing address: School of Chemistry and Molecular Biosciences, Building 76, University of
26 Queensland, Brisbane QLD 4072, Australia. Phone: +617 33653306; Fax: +617 33654699; E-
27 mail: m.schembri@uq.edu.au

28

29 **ABSTRACT**

30

31 The vacuolating autotransporter (AT) toxin (Vat) contributes to Uropathogenic *Escherichia coli*
32 (UPEC) fitness during systemic infection. Here we characterised Vat and investigated its
33 regulation in UPEC. We assessed the prevalence of *vat* in a collection of 45 UPEC urosepsis
34 strains and showed that it was present in 31 (68%) of the isolates. The isolates containing the *vat*
35 gene corresponded to three major *E. coli* sequence types (ST12, 73 and 95) and these strains
36 secreted the Vat protein. Further analysis of the *vat* genomic locus identified a conserved gene
37 located directly downstream of *vat* that encodes a putative MarR-like transcriptional regulator,
38 which we termed *vatX*. The *vat-vatX* genes were present in the UPEC reference strain CFT073
39 and RT-PCR revealed both genes are co-transcribed. Over-expression of *vatX* in CFT073 led to a
40 3-fold increase in *vat* gene transcription. The *vat* promoter region contained three putative
41 nucleation sites for the global transcriptional regulator H-NS; thus the *hns* gene was mutated in
42 CFT073 (to generate CFT073*hns*). Western blot analysis using a Vat-specific antibody revealed
43 a significant increase in Vat expression in CFT073*hns* compared to wild-type CFT073. Direct H-
44 NS binding to the *vat* promoter region was demonstrated using purified H-NS in combination
45 with electrophoresis mobility shift assays. Finally, Vat-specific antibodies were detected in
46 plasma samples from urosepsis patients infected by *vat*-containing UPEC strains, demonstrating
47 Vat is expressed during infection. Overall, this study has demonstrated that Vat is a highly
48 prevalent and tightly regulated immunogenic SPATE secreted by UPEC during infection.

49

50 **IMPORTANCE**

51

52 Uropathogenic *Escherichia coli* (UPEC) are the major cause of hospital and community acquired
53 urinary tract infections. The Vacuolating autotransporter toxin (Vat) is a cytotoxin known to
54 contribute to UPEC fitness during murine sepsis infection. In this study, Vat was found to be
55 highly conserved and prevalent among a collection of urosepsis clinical isolates, and expressed at
56 human core body temperature. Regulation of *vat* was demonstrated to be directly repressed by
57 the global transcriptional regulator H-NS and upregulated by the downstream gene *vatX* (a new
58 MarR-type transcriptional regulator). Additionally, increased Vat-specific IgG titres were

59 detected in plasma from corresponding urosepsis patients infected with *vat*-positive isolates.
60 Hence, Vat is a highly conserved and tightly regulated urosepsis-associated virulence factor.

61 INTRODUCTION

62

63 Urinary tract infections (UTIs) are one of the most common human infections, and affect 40-
64 50% of women and approximately 12% of men globally (1). UTIs are ascending infections and
65 can involve infection of the bladder (cystitis), kidneys (pyelonephritis) or dissemination into the
66 bloodstream (urosepsis). Uropathogenic *Escherichia coli* (UPEC) are the primary etiological
67 agent of UTI and cause 70-90 % of all such infections (2). UPEC can survive in the urinary tract
68 and cause disease due to a diverse range of virulence factors including fimbriae (3-6),
69 autotransporter (AT) proteins (7-10), surface polysaccharides such as the O-antigen and capsule
70 (11-13), iron acquisition systems (14-16) and toxins (17-21).

71

72 AT proteins constitute a large family of proteins from Gram-negative bacteria that are
73 translocated by a dedicated type V secretion system (reviewed in 22, 23-26). AT translocation
74 also requires accessory proteins including the β -barrel assembly module (BAM) and the
75 translocation and assembly module (TAM) (27-30). AT proteins consist of three major domains:
76 (i) a signal peptide that targets the protein to the secretory apparatus for inner membrane
77 translocation; (ii) a passenger domain that comprises the functional domain of the protein; and
78 (iii) a translocator domain that inserts into the outer membrane (reviewed in 22, 23, 25, 31-33) .

79 One major subgroup of AT proteins is the serine protease AT proteins of *Enterobacteriaceae*
80 (SPATEs). SPATEs are characterised by the presence of an immunoglobulin A1-like protease
81 domain (PF02395) within the passenger domain that contains the conserved serine protease motif
82 GDSGS (34, 35). The first serine within this motif comprises the catalytic triad in conjunction
83 with upstream conserved histidine and aspartate residues. SPATEs can be phylogenetically
84 grouped into two classes (reviewed in 34, 36, 37). Class I SPATEs represent the major group of
85 these proteins and exhibit cytotoxic activity (37-43). Class II SPATEs recognise a more diverse
86 range of substrates including mucins (reviewed in 34, 36, 37) and immunomodulatory host
87 proteins (44).

88

89 The vacuolating AT toxin (Vat) of *E. coli* is a class II SPATE (34, 36, 45) that exhibits
90 cytotoxicity to chicken embryonic fibroblast cells and contributes to avian cellulitis infection
91 (46). The *vat* gene was originally identified within a pathogenicity island (Vat-PAI) from the

92 avian pathogenic *E. coli* (APEC) strain Ec222 (46). The Vat-PAI is integrated into the Ec222
93 chromosome at the *thrW*-tRNA site between the *proA* and *yagU* genes (45, 46). The Vat-PAI
94 from Ec222 consists of 33 open reading frames (ORFs), with the *vat* gene residing at ORF#27.
95 Only five additional ORFs in this PAI were reported to share homology with other previously
96 known protein sequences. This includes the ORF located downstream of *vat* (ORF#26), which
97 shares 44% amino acid identity to the P pilus associated transcriptional regulatory protein PapX
98 from UPEC strain CFT073 (46). PapX belongs to the family of multiple antibiotic resistance
99 (MarR) regulators of *Enterobacteriaceae* and contributes to flagella regulation by binding to the
100 promoter region of the *flhDC* master regulator genes (47-49). In UPEC, the *vat* gene is
101 associated with virulence and contributes to survival during murine systemic infection (50).

102
103 The full-length Vat protein is ~140 kDa and is processed during translocation to release a 111.8
104 kDa passenger domain into the extracellular milieu. Vat shares 78% identity to the APEC
105 associated Temperature-sensitive hemagglutinin (Tsh), which is almost identical (99% amino
106 acid identity) to the SPATE Haemoglobin binding protein (Hbp) (51, 52). Hbp has been analysed
107 extensively in the *E. coli* intra-abdominal clinical strain EB1, and its crystal structure has been
108 solved (53, 54). Tsh/Hbp possess dual proteolytic and adhesive properties (55-57). Unlike
109 Tsh/Hbp, Vat is unable to digest casein at 37°C (45, 46).

110
111 Despite these functional differences, the high protein sequence identity shared between Tsh/Hbp
112 and Vat has led to confusion in the annotation of *vat* genes within *E. coli* genomes available on
113 the NCBI database. For example, the CFT073 *vat* gene (c0393) has been annotated as *hbp* (58),
114 and even referred to as *tsh* due to its temperature-dependent regulation (59). In addition, the *vat*
115 gene from UPEC strain 536 is annotated as *sepA*, which encodes the *Shigella* extracellular
116 protein A (45).

117
118 In this study, we have examined the sequence conservation of *vat* genes from available *E. coli*
119 genomes and compared its genomic location, with the aim to correct existing annotation errors
120 and *vat* nomenclature. We also examined the role of the putative MarR regulator identified
121 downstream of the *vat* gene as well as the histone-like nucleoid protein H-NS in regulation of the
122 *vat* gene. Finally, we examined the prevalence, expression and secretion of Vat in a collection of

123 UPEC urosepsis isolates, and investigated its immunogenicity by examining plasma from
124 urosepsis patients.

125

126 **MATERIALS AND METHODS**

127

128 **Ethics statement.** This study was performed in accordance with the ethical standards of The
129 University of Queensland, Princess Alexandra Hospital, Gold Coast Hospital, Queensland
130 Health, Griffith University and the Helsinki Declaration. The study was approved, and the need
131 for informed consent was waived by the institutional review boards of the Princess Alexandra
132 Hospital (2008/264), Queensland Health and Griffith University (MSC/18/10/HREC).

133

134 **Bacterial strains and growth conditions.** *E. coli* strains CFT073 (60), IHE3034 (61), 536 (62),
135 MG1655 (63) and BL21 (64), as well as the *E. coli* reference (ECOR) collection (65), have been
136 described previously. The 45 urosepsis UPEC strains were isolated from the blood of patients
137 presenting with urosepsis at the Princess Alexandra Hospital (Brisbane, Australia). A matching
138 urine sample was also cultured from each patient; in all cases the blood and urine isolates were
139 identical as determined by virulence gene profiling. Unless otherwise stated, strains used in this
140 study were routinely grown at 37°C on solid or in liquid Lysogeny broth (LB) supplemented
141 with antibiotics: kanamycin (kan [100µg/mL]), ampicillin (amp [100µg/mL]) or chloramphenicol
142 (cam [30µg/mL]). Supplementation of growth media with L-arabinose (0.2% [w/v]) or isopropyl
143 β-D-1-thiogalactopyranoside (IPTG [1mM]) was used to induce plasmid-mediated gene
144 expression.

145

146 **Bioinformatic analysis.** The presence of the *vat* gene was determined in 77 complete *E. coli*
147 genomes (listed in Table S1) available from the National Centre for Biotechnology Information
148 (NCBI) database by BLAST analysis using the *vat* gene (c0393) from the CFT073 genome
149 (Genbank accession no.: AE014075.1 (58)) as a search tool. The cut-off was set at >85% amino
150 acid identity of the encoded protein sequence. The genomic location surrounding the *vat* gene in
151 each of the *vat*-positive strains was investigated in Artemis (66). All *vat* genes identified were
152 located on a PAI defined by the *proA* and *yagU* genes. The nucleotide sequence of each *vat*-
153 associated PAI was compared in EasyFig (67).

154 A comparative protein analysis of the MarR family of transcriptional regulators (Table S2) was
155 performed to analyse their relative phylogenetic relationship to VatX. The MarR dataset was
156 compiled using an iterative approach that involved BLAST analysis against the 77 complete
157 NCBI *E. coli* genomes listed in Table S1. Representative protein sequences, underlined in Table
158 S2, were chosen for each MarR type regulator based on previous characterisation in the
159 literature. These sequences included MarR from MG1655 (b1530), MprA(EmrR) from MG1655
160 (b2684), HosA from E2348/69 (E2348C_3010), HpcR/ HpaR from strain W (WFL_22965),
161 SlyA from MG1655 (b1642) and PapX from CFT073 (c3582). Each of the representative
162 sequences were used to BLAST against the 77 complete *E. coli* genomes and 330 homologous
163 protein sequences were identified ($E < 0.001$). The evolutionary relationship between VatX and
164 other representative MarR regulators, as well as the protein sequences listed in Table S2, was
165 inferred using ClustalΩ (68, 69) and visualised through FigTree (70).

166

167 **DNA manipulation and genetic techniques.** DNA techniques were performed as previously
168 described (71). Isolation of plasmid DNA was performed using the QIAprep spin column
169 miniprep kit (QIAGEN). Polymerase chain reactions (PCR) were performed using the specified
170 primers which were sourced from Integrated DNA Technologies (Singapore). PCR products
171 were amplified using *Taq* DNA polymerase according to the manufacturer's instructions (New
172 England Biolabs). Sequencing reactions were performed using the BigDye Terminator v3.1 cycle
173 DNA sequencing kit as per the manufacturer's specifications (Applied Biosystems) and analysed
174 by the Australian Equine Genome Research Centre. Cloning reactions involving restriction
175 endonucleases were performed as per the manufacturer's instructions (New England Biolabs).

176

177 **Multi locus sequence typing (MLST) and PCR screening.** Prevalence of the *vat* gene was
178 assessed by PCR using primers 2020 (5'-GTATATGGGGGGCAACATAC-3') and 2021 (5'-
179 GTGTCAGAACGGAATTGTCG-3'), which were designed based on the sequence of the *vat*
180 gene from CFT073 (c0393). The *vat* gene sequence from ten of the 31 *vat*-positive UPEC
181 urosepsis strains was determined and deposited on the NCBI database (accession numbers:
182 PA11B *vat*, KR094926; PA15B *vat*, KR094927; PA32B *vat*, KR094928; PA38B *vat*,
183 KR094929; PA42B *vat*, KR094930; PA48B *vat*, KR094931; PA56B *vat*, KR094932; PA57B
184 *vat*, KR094933; PA60B *vat*, KR094934; PA66B *vat*, KR094935). The sequence type of the

185 UPEC urosepsis strains was determined using the seven-gene MLST scheme
186 (<http://mlst.ucc.ie/mlst/dbs/Ecoli>) (72). PCR was performed as follows: initial denaturation at
187 94°C for 5 m; 25 cycles of denaturation at 94°C for 30 s, annealing at 50°C for 30 s, extension at
188 72°C for 30 s followed by a final extension at 72°C for 7 m.

189

190 **Construction of deletion mutants.** The *vat* (c0393), *vatX* (c0392) and *hns* (c1701) genes were
191 mutated in CFT073 using λ -Red mediated homologous recombination (73). Briefly, the
192 kanamycin gene from pKD4 or the chloramphenicol gene from pKD3 were amplified using PCR
193 primers containing 50-bp flanking regions homologous to the target genes *vat* (3353: 5'-
194 TCGTAATGAACACAGTTCATCTGATCTCCACACACCAAGACTTGATAAGCTcagcttga
195 gcgattgtgtagg-3' and 3354: 5'-
196 GAAACCACCACCCCATGATTTTGTTTTACCGCTGTACAGGCCTGCTGACGCgacatgggaa
197 ttagccatggtcc-3'), *vatX* (5232: 5'-
198 TTCACGATACTTCATGTAACACTCAGGTTGAGTAATCTTCgtgtaggetggagctgcttc-3' and
199 5233: 5'-
200 AGAATACATTGTAAGAAGATGACTGTTAGTATGTTTTAACAcatatgaatatacctcctta-3') or
201 *hns* (1583: 5'-
202 TCGTGCGCAGGCAAGAGAATGTACACTTGAAACGCTGGAAGAAATGCTGGgtgtaggctg
203 gagctgcttc-3' and 1584: 5'-
204 TTGATTACAGCTGGAGTACGGCCCTGGCCAGTCCAGGTTTTAGTTTCGCCcatatgaatatacc
205 tccttag-3'). Amplified fragments were transformed into CFT073(pKD56) expressing of the λ -
206 Red recombinase in order to facilitate homologous recombination for inactivation deletion of the
207 target gene. Removal of the antibiotic resistance gene cassette was performed using plasmid
208 pCP20 as previously described, and enabled the construction of the CFT073*vatX hns* double
209 mutant.

210

211 **Construction of plasmids.** A segment of the *vat* gene corresponding to amino acid residues 63-
212 465 of the passenger domain was amplified from CFT073 using primers 1491 (5'-
213 tactccaatccaatgeTCCTTACCAGACATAACCGCG-3') and 1494 (5'-
214 ttatccacttccaatgTTACCCCGCATATTGATCATTGCC-3') and cloned as a 6 x histidine N-
215 terminal fusion into the pLicA vector using ligation independent cloning (designated pVat⁴⁰³).

216 The full-length *vat* gene (c0393) and the downstream gene *vatX* gene (c0392) were PCR
217 amplified from CFT073 using the following primer pairs; *vat*: 1524 (5'-
218 cgcgCTCGAGataataaggaattactATGAATAAAATATACGCTC-3') and 1525 (5'-
219 cgcgcaagcttCAAAGCAATAGTCCCTTTGC-3'); and *vatX*: 5244 (5'-
220 cgcgctcgagataataaggaaTCTTCATGAGTTTTCTTTTGCCGTGTGG-3') and 5245 (5'-
221 cccggaagcttTCAATTAACATTAAGGTTTGATA-3'). The PCR products were purified and
222 cloned into XhoI-HindIII digested pSU2718 to generate the plasmids pVat and pVatX.
223 Transcription of the *vat* and *vatX* genes in these plasmids was regulated by the *lac* promoter (74).

224
225 **Comparative quantitative reverse transcriptase PCR (qRT-PCR).** Comparative qRT-PCR
226 was performed essentially as previously described (47). Briefly, strains CFT073, CFT073*vatX*
227 and CFT073*vatX* (pVatX) were grown in LB broth (supplemented with IPTG) until exponential
228 growth phase. The total RNA from each strain was extracted using the RNeasy mini kit as per
229 manufacturer's instructions (QIAGEN). Samples were subjected to RNase free DNA digestion
230 and first strand cDNA synthesis was performed using SuperscriptIII (Invitrogen Life
231 Technologies) with random hexamer (50ng/μL) primers (Invitrogen Life Technologies).
232 Residual RNA was digested by RNaseH and samples were re-purified as recommended by the
233 manufacturer (QIAGEN). The ViiA 7 instrument and software (v 1.2.1) was used to carry out RT
234 PCR reactions (95°C 10 s; 95°C 15 s, 60°C 15 s and 72°C 30 s for 40 cycles). Primers specific to
235 the *vat* gene (5470: 5'-TACCGTAACCAGCTCATCAACAG-3' and 5471: 5'-
236 CATACCACCTGTTACCCAATGT-3') and *gapA* (control; 820: 5'-
237 GGTGCGAAGAAAGTGGTTATGAC-3' and 821: 5'-GGCCAGCATATTTGTCTGAAGTTAG-
238 3') were used to amplify transcripts with SybrGreenI (5 μL) master mix (Applied Biosystems).
239 Each reaction was performed in triplicate and a subsequent melt curve was generated for
240 validation of the results (95°C 15 s, 60°C 1 m and 95°C for 10 s). Cycle threshold values
241 obtained were normalised to the endogenous control and the $2^{-\Delta\Delta Ct}$ method (75) was applied for
242 the comparative analysis. The resulting ratios were statistically analysed using a one-way
243 ANOVA. All experiments were performed in triplicate.

244
245 **5' RACE and Virtual Footprint analysis.** The transcriptional start site for *vat* was determined
246 using the 5' RACE system for rapid amplification of cDNA ends (version 2.0, Invitrogen Life

247 Technologies) following the manufacture's specifications. Two gene specific primers (5863: 5'-
248 ATGCAGATAGTGCCAGAG-3' and 5864: 5'-CTCTGCGGGTACTCCCTTAC-3') were
249 used. Putative DNA binding motifs in the *vat* promoter region were identified using Virtual
250 Footprint software (76).

251
252 **Electrophoretic mobility shift assay (EMSA).** EMSA was performed essentially as described
253 previously (77) but with minor adaptations. Briefly, four individual fragments (152 bp, 218 bp,
254 312 bp and 479 bp) were PCR amplified from the plasmid pBR322 (152 bp: 5'-
255 CATTGGACCGCTGATCGT-3' and 5'-CTTCCATTCAGGTCGAGGT-3'; 218 bp: 5'-
256 AATATTATTGAAGCATTATCAGGGTTA-3' and 5'-
257 ATGATAAGCTGTCAAACATGAGA-3'; 312 bp: 5'-TATCGACTACGCGATCATGG-3' and
258 5'-TCTCCCTTATGCGACTCCTG-3'; and 479 bp: 5'-GACCGATGCCCTTGAGAG-3' and 5'-
259 GATCGAAGTTAGGCTGGTAAGA-3'). The 218-bp fragment containing the H-NS repressed
260 *bla* gene promoter was included in the assay as a positive control, while the remaining three
261 fragments do not bind H-NS. The *vat* gene promoter region (252 bp) encompassing all three of
262 the putative H-NS binding sites identified, was also PCR amplified (6103: 5'-
263 CCTGAGAAAAGCAAACAACA-3' and 6104: 5'-TTTTAGAGCGTATATTTTATTCAT-3')
264 from the genomic DNA of CFT073. This 252-bp fragment was added in an equimolar ratio with
265 the control fragments (7.5 nM per fragment [\sim 100 ng]). Purified native H-NS protein was added
266 to each reaction in increasing concentrations (0 μ M, 0.1 μ M, 0.5 μ M and 1.0 μ M). Reactions
267 were incubated at room temperature (15 min in H-NS binding buffer to allow for protein-DNA
268 complex formation. Samples were examined by high-resolution agarose gel electrophoresis (3%
269 Lonza Metaphor [50 V at 4°C]), and viewed under ultraviolet light after staining with ethidium
270 bromide (0.5 μ g/ mL). Invitrogen's 1 kbp+ ladder was used as a molecular marker.

271
272 **Preparation of supernatant proteins.** Bacterial cultures (10 mL) were standardised to an
273 optical density at 600nm equal to 1.0 ($OD_{600} = 1.0$), centrifuged (2057 x g), and the supernatant
274 was collected and filtered (0.22 μ m). Proteins were precipitated by the addition of 10%
275 trichloroacetic acid (TCA) overnight at 4°C. Following precipitation, supernatant fractions were
276 concentrated by centrifugation (12,100 x g) and washed twice with 80% acetone to remove
277 residual TCA. Proteins were resuspended in a final volume of 0.1 mL (100-fold concentration).

278

279 **Purification of denatured His-tagged Vat protein.** A bacterial culture (200mL) of *E. coli*
280 BL21 λ DE3 expressing the truncated Vat⁴⁰³ protein encoded on plasmid pVat⁴⁰³ was grown in
281 LB. Bacterial cells were pelleted by centrifugation (2057 x g) and lysed (7M urea, 0.1 M
282 NaH₂PO₄, 0.01 M Tris·Cl [pH 8.0]). The recombinant Vat⁴⁰³ protein was purified under
283 denaturing conditions using QIAGEN's Ni-NTA spin column kit. The cleared lysate was passed
284 through a pre-equilibrated column via centrifugation (270 x g) to allow for the 6xHis tagged-Vat
285 protein to bind. The column was washed (0.1 M NaH₂PO₄, 0.01 M Tris·Cl ([pH 6.3]) and the
286 bound Vat protein was eluted (0.1 M NaH₂PO₄, 0.01 M Tris·Cl [pH 4.5]) by centrifugation (890
287 x g). Protein concentrations were determined using the bicinchoninic acid protein assay kit as per
288 the manufacturer's instructions (Thermo Scientific Pierce Biotechnology). Purity of the eluted
289 protein was validated by sodium-dodecyl-disulfide polyacrylamide gel electrophoresis (SDS-
290 PAGE) analysis (12% polyacrylamide gel) and Coomassie staining.

291

292 **Immunoblotting.** The purified His-tagged recombinant Vat protein was used to generate a Vat-
293 specific polyclonal antibody following a standard protocol (Institute of Medical and Veterinary
294 Science, South Australia). Concentrated supernatant proteins were re-suspended in 50 μ L of SDS
295 loading buffer (100 mM Tris-HCl, 4% w/v SDS, 20% w/v glycerol, 0.2% w/v bromophenol blue,
296 pH 6.8) and a 10 μ L sample was boiled for 10 min prior to SDS-PAGE. SDS-PAGE and transfer
297 of proteins to a PVDF membrane for western blot analysis was performed as previously
298 described (78). Anti-Vat polyclonal antibodies were used as the primary antibody, and alkaline
299 phosphatase conjugated anti-rabbit antibodies (Sigma Aldrich) were used as the secondary
300 antibody. SIGMAFASTTM BCIP®/NBT (Sigma-Aldrich) was used as the substrate for detection.

301

302 **Human plasma samples and measurement of Vat immunogenicity.** Blood plasma (collected
303 within 4 days post-admission) and matching clinical isolates were obtained from 45 urosepsis
304 patients admitted to the Princess Alexandra Hospital (Brisbane, Australia). The clinical strains
305 isolated from each urosepsis patient were grouped as Vat positive (Vat+) and Vat-negative (Vat-)
306 according to the prevalence of the *vat* gene, as determined by PCR screening using *vat* specific
307 primers. A negative control group of plasma samples was independently obtained from 42
308 healthy volunteers with no recent history of UTI. The ELISA assay was performed using Nunc

309 MaxiSorp flat-bottom 96 well microtiter plates (Thermo Scientific). Each well was coated with
310 recombinant Vat protein (10 µg/ml) using carbonate coating buffer (18 mM Na₂CO₃, 450 mM
311 NaHCO₃, pH 9.3 [4°C, overnight]). Plates were washed twice with 0.05% v/v Tween20 PBS
312 (PBST) and blocked with 5% w/v skim milk in PBST (150 µl) for 90 min at 37°C. Each well
313 was then washed four times with PBST prior to incubation (90 min at 37°C) with individual
314 plasma samples (1:10 dilution). Unbound antibodies were removed by washing with PBST.
315 Peroxidase-conjugated anti-human IgG (1:30,000 dilution in 5% skim milk) was applied as a
316 secondary antibody for detection (incubated at 37°C for 90 min). Plates were washed four times
317 with PBST and bound anti-human IgG was detected using 3,3',5,5'-tetramethylbenzidine as a
318 substrate. Reactions were stopped with 1 M HCl. The absorbance of each well was measured at
319 450 nm using the Spectramax plus³⁸⁴ plate reader via the SoftMax Pro[®]v5 program. Data
320 obtained was analysed using GraphPrism5 software and a one-way ANOVA statistical analysis
321 was performed.

322

323 RESULTS

324

325 **The *vat* gene is located on a pathogenicity island at a conserved genomic location.** The
326 prevalence of *vat* was assessed in 77 complete *E. coli* genomes available on the NCBI database
327 (Table S1). The *vat* gene was identified in 14 of these strains; these included the previously
328 characterised *vat*-positive UPEC strains CFT073 and 536, as well as twelve additional strains
329 from which *vat* has not previously been characterised (APEC O1, NRG 857C, LF82, IHE3034,
330 S88, 83972, PMV-1, clone D i2, clone D i14, ATCC 25922, Nissle 1917 and UM146). In all 12
331 strains, the *vat* gene was part of a pathogenicity island (PAI) flanked by the *proA* and *yagU*
332 genes relative to the *E. coli* K12 MG1655 chromosome. This genomic location is consistent with
333 the original identification of *vat* in APEC strain Ec222 (46). Closer examination of the genomic
334 context of *vat* revealed that the upstream region (i.e. the *yagU* end) is highly conserved. In
335 contrast, the region downstream of *vat* (i.e. the *proA* end) exhibits extensive variation, with a
336 range of different DNA segments inserted at various positions of the PAI in strains APEC O1,
337 83972, UM146, 536 and Ec222 (Fig. 1A).

338

339 **Vat is secreted by several genome sequenced UPEC strains.** The secretion of Vat following
340 growth in LB broth at 37°C was assessed from a selection of the *vat*-positive UPEC strains
341 described above (i.e. CFT073, IHE3034 and 536). As a positive control, the *vat* gene from
342 CFT073 was amplified by PCR, cloned into the low copy number expression vector pSU2718 to
343 generate the plasmid pVat, and transformed into *E. coli* MG1655 to generate the recombinant
344 strain MG1655(pVat). Western blot analysis using a Vat-specific antibody detected a single band
345 of ~110 kDa that corresponded to the predicted size of the secreted passenger domain of Vat in
346 the supernatant of MG1655(pVat), but not the vector control strain MG1655(pSU2718) (Fig.
347 1B). The *vat* gene was also mutated in CFT073 to generate null mutant strain CFT073*vat*. SDS-
348 PAGE and western blot analysis of the supernatant fraction obtained from CFT073 and
349 CFT073*vat* using our Vat-specific antibody identified the secreted Vat passenger domain from
350 CFT073 but not CFT073*vat* (Fig. 1B). Finally, we also detected bands corresponding to the Vat
351 passenger domain in the supernatant fraction prepared from strains IHE3034 and 536. Taken
352 together, our data demonstrate that Vat is expressed and secreted by the genome-sequenced
353 strains CFT073, IHE3034 and 536.

354

355 **A *marR*-like gene is located immediately downstream of the *vat* gene.** We were interested to
356 study the regulation of Vat, and noted a small open reading frame located directly downstream of
357 the *vat* gene in all *vat*-positive strains (Fig. 1A). This gene, which we have termed *vatX*,
358 corresponds to c0392 in CFT073 (58) and ORF#26 in the Vat PAI from Ec222 (46). The VatX
359 protein sequence is highly conserved (99% amino acid identity in the 14 *vat*-positive completely
360 sequenced strains described above) and shares 44% amino acid identity with the CFT073 P pilus-
361 associated transcriptional regulator PapX. Further analysis of VatX revealed it contains a MarR
362 PFAM domain (PF01047) and a helix-turn-helix motif characteristic of DNA binding proteins.
363 To examine the relationship between VatX and other regulator proteins, we generated a dataset
364 comprising previously characterised *E. coli* MarR type regulators (Table S2) (47, 79-82). A
365 multiple sequence alignment using representative regulator protein sequences (Fig. 2) as well as
366 a more detailed phylogenetic analysis of all MarR-like sequences identified in the 77 complete *E.*
367 *coli* genomes described above (Fig S1) revealed that VatX forms a distinct clade within the
368 MarR regulator family, and is most closely related to the PapX, SfaX and FocX fimbriae-
369 associated regulators (47, 80, 83, 84).

370

371 **Expression of the *vat* gene is upregulated by VatX.** The proximity, orientation and conserved
372 genetic organization of the *vat* and *vatX* genes led us to examine if VatX contributes to the
373 regulation of the *vat* gene. In order to study this, we generated a CFT073 *vatX* mutant
374 (CFT073*vatX*) and examined the transcription of *vat* in CFT073 and CFT073*vatX* using
375 comparative qRT-PCR. In addition, the *vatX* gene from CFT073 was PCR amplified and cloned
376 into the pSU2718 expression vector (to generate the plasmid pVatX) and used to complement the
377 CFT073*vatX* mutant. No significant difference was observed in the level of *vat* mRNA
378 transcribed in CFT073 and CFT073*vatX* following growth in LB broth at 37°C (Fig. 3A).
379 However, the over-expression of VatX in CFT073*vatX* (pVatX) resulted in an approximately 3-
380 fold higher level of *vat* mRNA transcript compared to WT CFT073 (Fig. 3A). To explore the
381 effect of VatX on Vat expression further, we compared the level of Vat secreted into the
382 supernatant fraction by CFT073, CFT073*vatX* and CFT073*vatX*(pVatX) by western blot analysis
383 (Fig 3B). Consistent with our transcriptional data, the over-expression of VatX in
384 CFT073*vatX*(pVatX) resulted in a significantly increased level of Vat in the culture supernatant,
385 while no difference in the level of secreted Vat was observed in CFT073 and CFT073*vatX*. A
386 similar increase in secreted Vat was also observed when WT CFT073 was transformed with
387 plasmid pVatX (i.e. strain CFT073[pVatX]) (Fig. 3B). Taken together, our results demonstrate
388 that while deletion of *vatX* does not alter the level of Vat secretion, its over-expression
389 significantly enhances Vat expression.

390

391 **Transcription of the *vat* gene is directly repressed by H-NS.** Given the regulatory effect
392 exhibited by VatX on *vat* transcription, we investigated the promoter region of the *vat* gene to
393 identify putative binding sites for other transcription factors. The transcriptional start site for *vat*
394 was determined using 5' RACE and was mapped to a position 80-bp upstream of the Vat ATG
395 start codon. Consensus -35 (5'-ATCACA-3') and -10 (5'-ATTAAT-3') promoter sequence
396 elements, separated by an 18-bp spacer region, were identified upstream of this site (Fig. 4A).
397 Virtual footprint software was used to analyse the *vat* promoter region for putative regulatory
398 binding sites. From this *in silico* analysis, two putative H-NS nucleation sites were identified on
399 the anti-sense strand overlapping the 18-bp spacer region and the 5' end of the -35 element. A

400 third H-NS nucleation site was determined on the direct strand 10-bp downstream of the
401 transcriptional start site.

402

403 The global transcriptional regulator H-NS is known to bind to curved and A-T rich DNA
404 sequences upstream of several defined UPEC virulence genes (85), including genes encoding for
405 toxins (86-89) and autotransporter proteins (8, 10, 90). To investigate the effect of H-NS on *vat*
406 transcription, the level of Vat expression was compared by western blot analysis of supernatant
407 fractions prepared from WT CFT073, CFT073*vat*, CFT073*vatX*, CFT073*hns* and a CFT073*vatX*
408 *hns* double mutant (Fig. 4B). The amount of Vat secreted by CFT073*hns* and CFT073*vatX hns*
409 was markedly increased compared to WT CFT073. Consistent with previous results, the level of
410 Vat detected in supernatant fraction of CFT073*vatX* was similar to that detected from WT
411 CFT073.

412

413 **H-NS binds to the *vat* promoter region.** To further investigate the role of H-NS in repression of
414 *vat* transcription, an EMSA was performed using increasing concentrations of native H-NS
415 protein and the 252bp PCR amplified region of the *vat* gene promoter possessing the three
416 potential H-NS binding sites (Fig 4C). As a positive control, the *bla* gene promoter from the
417 cloning vector pBR322 was also PCR amplified and included in the assay; H-NS is known to
418 bind to this DNA fragment (91). Three additional fragments amplified from regions of pBR322
419 known not to bind H-NS were included in the assay as negative controls. In our experiment, H-
420 NS bound with strong affinity to the DNA fragment corresponding to the *vat* gene promoter.
421 Indeed, this binding affinity was stronger than that observed for the DNA fragment containing
422 the control *bla* gene promoter. No binding of H-NS was observed to the negative control DNA
423 fragments, demonstrating the specificity of H-NS binding in this assay.

424

425 **The *vatX* gene is co-transcribed with *vat*.** H-NS regulates the transcription of several UPEC
426 genes by competing for binding to their promoter element with a MarR-type regulatory protein;
427 this includes SfaX binding to the *sfaH* fimbrial promoter (80), PapX binding to the *flhDC* flagella
428 master regulator promoter (92), and SlyA binding to the type 1 fimbriae *fimB* recombinase
429 promoter (93). The SfaX and PapX regulators are co-transcribed as part of their respective
430 upstream fimbrial operon (encoding S and P type fimbriae, respectively (47, 80)). Taking this

431 into consideration, we employed RT-PCR analysis to test for transcription of the *vat* and *vatX*
432 genes as a single mRNA in CFT073. Due to the increased amount of Vat protein secreted by the
433 CFT073*hns* mutant strain (as shown by Western blot analysis), total RNA was extracted from
434 this strain, converted to cDNA and screened for a *vat-vatX* nucleic acid fragment using internal
435 primers specific for both genes by RT-PCR (Fig. 4D). For comparison, an additional set of
436 primers were used to amplify the *vatX* gene alone. Bands corresponding to the predicted sizes
437 determined for the *vatX* and the *vat-vatX* transcripts were amplified from CFT073*hns* cDNA.
438 Thus, while we cannot rule out the presence of an independent promoter upstream of *vatX*, our
439 results demonstrate that the *vat-vatX* genes are co-transcribed in the absence of H-NS.

440

441 **Vat is prevalent, highly conserved and is secreted by UPEC urosepsis isolates.** The *vat* gene
442 has previously been shown to be most prevalent in *E. coli* strains from the B2 phylogenetic
443 group, with a similar distribution observed among cystitis, pyelonephritis, prostatitis and
444 bloodstream isolates (45). Based on the observation that *vat* is required for UPEC fitness in a
445 mouse model of systemic infection (50), we screened a collection of urosepsis strains for the *vat*
446 gene by PCR. The *vat* gene was identified in 68% (31/45) of the urosepsis strains. MLST
447 analysis revealed strains from ST73, ST12 and ST95 were most predominant in this collection
448 (Fig. 5). Furthermore, supernatant fractions produced by these strains were examined by Western
449 blotting to analyse the expression and secretion of Vat following growth in LB at 37°C. For all
450 strains, a band corresponding to the Vat passenger domain hybridised with the Vat-specific
451 polyclonal antibody. The sequence of the *vat* gene was determined from *vat*-positive strains
452 representing each ST and found to be highly conserved ($\geq 97\%$ amino acid identity [Fig. 5]).
453 Minor sequence variations occurred at six locations within the passenger domain of the protein.
454 These residues were located within two regions in the Vat passenger domain (Fig. 5), both of
455 which are distal to the serine protease catalytic motif based on a structural model built using the
456 Hbp passenger domain (Fig. S2).

457

458 **The presence of *vat* is associated with increased anti-Vat IgG produced during infection.**
459 The high prevalence of *vat* in the UPEC urosepsis strains examined in this study, in combination
460 with its secretion during *in vitro* growth, prompted us to examine if an immunological response
461 against Vat was elicited during infection. To test this, an ELISA assay was performed using

462 blood plasma samples collected from the same urosepsis patients from which the urosepsis
463 strains were collected (Fig. 6). The blood plasma samples were examined for the presence of
464 Vat-specific IgG antibodies using purified recombinant Vat protein. The urosepsis patients were
465 divided into two groups; those infected with a *vat*-positive UPEC strain (n=31) and those
466 infected with a *vat*-negative UPEC strain (n=14). As an additional control, 42 plasma samples
467 collected from age and sex matched healthy individuals were also examined for an
468 immunological response against the Vat protein. In this assay, we observed a significant
469 difference ($P < 0.05$) in the anti-Vat IgG plasma titre in patients infected with a *vat*-positive
470 strain compared to a *vat*-negative strain or healthy individuals. Taken together, these data
471 suggest that Vat is a highly conserved immunogenic protein that is expressed by many UPEC
472 isolates during infection.

473

474 **DISCUSSION**

475

476 UPEC strains possess an array of virulence factors that are critical for their ability to cause
477 disease in extra-intestinal niches such as the urinary tract and the bloodstream (94, 95). Vat is a
478 member of the SPATEs that contributes to fitness of *E. coli* during systemic infection (46, 50). In
479 this study, we performed a comprehensive bioinformatic and molecular analysis of the *vat* gene.
480 We defined the transcriptional regulation of *vat* and demonstrated its immunogenicity using
481 plasma samples from urosepsis patients.

482

483 The genomic location of the *vat* gene was examined in all *vat*-positive completely sequenced *E.*
484 *coli* strains available on the NCBI database. The *vat* gene was shown to reside within the *thrW*-
485 PAI, downstream of *proA* and upstream of *yagU* relative to the *E. coli* MG1655 chromosome.
486 This is consistent with a previous report that examined the presence of *vat* in UPEC strains
487 CFT073 and 536, as well as the neonatal meningitis strain RS218 (45). The gene content of the
488 *vat*-containing *thrW*-PAI was conserved in the majority of strains examined, although some
489 differences were noted in strains Ec222, APEC-O1, 83972, UM146 and 536. Overall, our
490 bioinformatic analysis revealed that the *vat* gene (and the co-located *vatX* regulator gene) is
491 present in a range of different *E. coli* pathotypes.

492

493 Several studies have previously assessed the prevalence of the *vat* gene in *E. coli*. A study
494 conducted by Parham *et al* (45) reported a high prevalence of *vat* in group B2 phylogenetic
495 strains of the ECOR collection. A high frequency of the *vat* gene has also been observed in B2
496 strains associated with cystitis, pyelonephritis and prostatitis (45, 59), and *vat* has been strongly
497 associated with avian pathogenic *E. coli* (APEC) (96). Our analysis identified the *vat* gene in
498 68% of urosepsis isolates (n = 45). We also demonstrated that the sequence of *vat* is highly
499 conserved within a selection of strains representative of each of the ten different sequence types
500 identified in our collection. At the amino acid level, minor sequence variations were located
501 within two regions (VR1: S⁵²⁰-K⁵²⁹ and VR2: E⁷⁸³-V⁸²³) of the Vat passenger domain. However,
502 the canonical serine protease domain that is important for the catalytic function of SPATEs was
503 conserved in all ten of the Vat sequences analysed. Western blotting was also performed to
504 examine Vat expression, and revealed that Vat is expressed and secreted by all of the urosepsis
505 strains examined when grown at human core body temperature. Further investigation is required
506 to determine whether the minor sequence changes observed in Vat are associated with
507 corresponding differences in its cytotoxic properties.

508

509 Bioinformatic analysis identified a gene encoding a putative MarR-like transcriptional regulator
510 immediately downstream of *vat* (i.e. *vatX*). Although mutation of *vatX* did not result in a
511 detectable change in *vat* transcription or translation, overexpression of VatX via the introduction
512 of a plasmid containing the *vatX* gene (pVatX) was shown to positively regulate *vat*, resulting in
513 a 3-fold increase in *vat* transcription and a significant increase in the level of secreted Vat
514 protein. This data was suggestive of a more complex regulatory control of the *vat* gene. We
515 therefore mapped the promoter of *vat*, and identified several putative H-NS binding sites
516 proximal to this region. H-NS is a histone-like DNA-binding protein that shows affinity for A-T
517 rich and bent nucleation sites on DNA (97). In *E. coli*, H-NS has been shown to regulate multiple
518 genes, including genes associated with virulence, pH, osmoregulation and temperature sensing
519 (98-101). Our EMSA data revealed a strong interaction between H-NS and a 252-bp region of
520 the *vat* promoter that contains three putative H-NS binding sites. A role for H-NS in *vat*
521 regulation was subsequently demonstrated through the examination of a CFT073*hns* mutant,
522 which secreted a significantly higher level of Vat compared to the parent CFT073 strain. Taken

523 together, these results demonstrate that the regulation of *vat* is coordinated by both VatX and H-
524 NS, and further highlights the role of H-NS in the regulation of UPEC virulence factors (8, 9).

525
526 The MarR family of transcriptional regulators control the expression of multiple different genes,
527 including virulence factors, often in response to environmental stress (reviewed in 102, 103).
528 Bioinformatic analysis of MarR-type regulators from 77 completely sequenced *E. coli* genomes
529 revealed a high level of amino acid sequence conservation for proteins in each clade, but
530 significant variation between MarR regulators from different clades. VatX clustered as a separate
531 clade and is most closely related to PapX. Interestingly, the proteins encoding for other fimbrial
532 associated MarR-type regulators were also found within the PapX clade (Fig S1). Despite their
533 association with different fimbriae, these regulatory proteins are highly conserved ($\geq 97\%$ amino
534 acid identity). Some strains such as *E. coli* 536, 83972 and Nissle 1917 possess three or more
535 chromosomal copies of *papX* (Table S2). PapX regulates UPEC motility by repressing
536 transcription of the *flhDC* master regulator genes (47). We investigated the potential for VatX to
537 repress flagella-mediated motility of CFT073. However, no significant difference in motility was
538 observed between WT CFT073, CFT073*vatX* and the complemented CFT073*vatX* (pVatX)
539 mutant strains after growth at 28°C and 37°C (data not shown). The FliC major flagellin subunit
540 was also produced at a similar level in all three strains as determined by immunoblotting (data
541 not shown). Taken together, our data has identified VatX as a new member of the MarR type
542 family that appears to regulate *vat* in concert with H-NS. Further work is now required to map
543 the direct binding of VatX to the *vat* gene promoter, and to examine the competitive interplay
544 between VatX and H-NS in the regulation of *vat* transcription.

545
546 In a recent study using high-throughput transposon mutagenesis screening (50), the *vat* gene was
547 shown to contribute to survival of the UPEC strain CFT073 in the bloodstream of mice. This,
548 together with the observation that many urosepsis strains secrete Vat, prompted us to examine
549 the immunoreactivity of Vat in urosepsis patients. We detected a significant increase in Vat-
550 specific IgG titre in the plasma of urosepsis patients infected with *vat*-positive UPEC strains
551 compared to plasma from patients infected with *vat*-negative strains and healthy controls.
552 Although we cannot rule out that the responses we detected may in part be due to previous or
553 ongoing infection that culminated in sepsis, overall the data is consistent with the notion that Vat

554 is expressed during infection and elicits a strong immune response in some patients. Further
555 work is now required to understand the role of Vat during human infection and its cytotoxicity
556 profile.

557

558 **ACKNOWLEDGEMENTS**

559 We thank David Looke, Joan Faoagali and other members of the Microbiology Lab, Princess
560 Alexandra Hospital, for the collection of urosepsis strains and plasma samples, and Barbara
561 Johnson for the collection of patient clinical data. This work was supported by a grant from the
562 National Health and Medical Research Council (NHMRC) of Australia (APP1042651). MAS is
563 supported by an NHMRC Senior Research Fellowship (APP1106930), SAB by an NHMRC
564 Career Development Fellowship (APP1090456), GCU by an Australian Research Council
565 (ARC) Future Fellowship (FT110101048) and MT by an ARC Discovery Early Career
566 Researcher Award (DE130101169).

567 REFERENCES

- 568 1. **Foxman B.** 2010. The epidemiology of urinary tract infection. *Nat Rev Urol* **7**:653-660.
- 569 2. **Hooton TM, Stamm WE.** 1997. Diagnosis and treatment of uncomplicated urinary tract
570 infection. *Infect Dis Clin North Am* **11**:551-581.
- 571 3. **Connell H, Agace W, Klemm P, Schembri M, Marild S, Svanborg C.** 1996. Type 1
572 fimbrial expression enhances *Escherichia coli* virulence for the urinary tract. *Proc Natl*
573 *Acad Sci U S A* **93**:9827-9832.
- 574 4. **Mulvey MA, Lopez-Boado YS, Wilson CL, Roth R, Parks WC, Heuser J, Hultgren**
575 **SJ.** 1998. Induction and evasion of host defenses by type 1-piliated uropathogenic
576 *Escherichia coli*. *Science* **282**:1494-1497.
- 577 5. **Wu XR, Sun TT, Medina JJ.** 1996. *In vitro* binding of type 1-fimbriated *Escherichia*
578 *coli* to uroplakins Ia and Ib: relation to urinary tract infections. *Proc Natl Acad Sci U S A*
579 **93**:9630-9635.
- 580 6. **Roberts JA, Marklund BI, Ilver D, Haslam D, Kaack MB, Baskin G, Louis M,**
581 **Mollby R, Winberg J, Normark S.** 1994. The Gal(alpha 1-4)Gal-specific tip adhesin of
582 *Escherichia coli* P-fimbriae is needed for pyelonephritis to occur in the normal urinary
583 tract. *Proc Natl Acad Sci U S A* **91**:11889-11893.
- 584 7. **Ulett GC, Valle J, Beloin C, Sherlock O, Ghigo JM, Schembri MA.** 2007. Functional
585 analysis of antigen 43 in uropathogenic *Escherichia coli* reveals a role in long-term
586 persistence in the urinary tract. *Infect Immun* **75**:3233-3244.
- 587 8. **Allsopp LP, Beloin C, Ulett GC, Valle J, Totsika M, Sherlock O, Ghigo JM,**
588 **Schembri MA.** 2012. Molecular Characterization of UpaB and UpaC, Two New
589 Autotransporter Proteins of Uropathogenic *Escherichia coli* CFT073. *Infect Immun*
590 **80**:321-332.
- 591 9. **Allsopp LP, Totsika M, Tree JJ, Ulett GC, Mabbett AN, Wells TJ, Kobe B, Beatson**
592 **SA, Schembri MA.** 2010. UpaH Is a Newly Identified Autotransporter Protein That
593 Contributes to Biofilm Formation and Bladder Colonization by Uropathogenic
594 *Escherichia coli* CFT073. *Infect Immun* **78**:1659-1669.
- 595 10. **Totsika M, Wells TJ, Beloin C, Valle J, Allsopp LP, King NP, Ghigo JM, Schembri**
596 **MA.** 2012. Molecular Characterization of the EhaG and UpaG Trimeric Autotransporter
597 Proteins from Pathogenic *Escherichia coli*. *Appl Environ Microbiol* **78**:2179-2189.
- 598 11. **Anderson GG, Goller CC, Justice S, Hultgren SJ, Seed PC.** 2010. Polysaccharide
599 capsule and sialic acid-mediated regulation promote biofilm-like intracellular bacterial
600 communities during cystitis. *Infect Immun* **78**:963-975.
- 601 12. **Sarkar S, Ulett GC, Totsika M, Phan MD, Schembri MA.** 2014. Role of capsule and
602 O antigen in the virulence of uropathogenic *Escherichia coli*. *PLoS One* **9**:e94786.
- 603 13. **Phan MD, Peters KM, Sarkar S, Lukowski SW, Allsopp LP, Gomes Moriel D,**
604 **Achard ME, Totsika M, Marshall VM, Upton M, Beatson SA, Schembri MA.** 2013.
605 The serum resistome of a globally disseminated multidrug resistant uropathogenic
606 *Escherichia coli* clone. *PLoS Genet* **9**:e1003834.
- 607 14. **Valdebenito M, Bister B, Reissbrodt R, Hantke K, Winkelmann G.** 2005. The
608 detection of salmochelin and yersiniabactin in uropathogenic *Escherichia coli* strains by a
609 novel hydrolysis-fluorescence-detection (HFD) method. *Int J Med Microbiol* **295**:99-107.
- 610 15. **Garcia EC, Brumbaugh AR, Mobley HLT.** 2011. Redundancy and Specificity of
611 *Escherichia coli* Iron Acquisition Systems during Urinary Tract Infection. *Infect Immun*
612 **79**:1225-1235.

- 613 16. **Watts RE, Totsika M, Challinor VL, Mabbett AN, Ulett GC, De Voss JJ, Schembri**
614 **MA.** 2012. Contribution of siderophore systems to growth and urinary tract colonization
615 of asymptomatic bacteriuria *Escherichia coli*. *Infect Immun* **80**:333-344.
- 616 17. **Guyer DM, Radulovic S, Jones FE, Mobley HL.** 2002. Sat, the secreted autotransporter
617 toxin of uropathogenic *Escherichia coli*, is a vacuolating cytotoxin for bladder and
618 kidney epithelial cells. *Infect Immun* **70**:4539-4546.
- 619 18. **Rippere-Lampe KE, O'Brien AD, Conran R, Lockman HA.** 2001. Mutation of the
620 gene encoding cytotoxic necrotizing factor type 1 (cnf(1)) attenuates the virulence of
621 uropathogenic *Escherichia coli*. *Infect Immun* **69**:3954-3964.
- 622 19. **Dhokal Bijaya K, Mulvey Matthew A.** 2012. The UPEC Pore-Forming Toxin α -
623 Hemolysin Triggers Proteolysis of Host Proteins to Disrupt Cell Adhesion, Inflammatory,
624 and Survival Pathways. *Cell Host & Microbe* **11**:58-69.
- 625 20. **Garcia TA, Ventura CL, Smith MA, Merrell DS, O'Brien AD.** 2013. Cytotoxic
626 necrotizing factor 1 and hemolysin from uropathogenic *Escherichia coli* elicit different
627 host responses in the murine bladder. *Infect Immun* **81**:99-109.
- 628 21. **Smith YC, Rasmussen SB, Grande KK, Conran RM, O'Brien AD.** 2008. Hemolysin
629 of uropathogenic *Escherichia coli* evokes extensive shedding of the uroepithelium and
630 hemorrhage in bladder tissue within the first 24 hours after intraurethral inoculation of
631 mice. *Infect Immun* **76**:2978-2990.
- 632 22. **Leyton DL, Rossiter AE, Henderson IR.** 2012. From self sufficiency to dependence:
633 mechanisms and factors important for autotransporter biogenesis. *Nat Rev Microbiol*
634 **10**:213-225.
- 635 23. **Leo JC, Grin I, Linke D.** 2012. Type V secretion: mechanism(s) of autotransport
636 through the bacterial outer membrane. *Philos Trans R Soc Lond B Biol Sci* **367**:1088-
637 1101.
- 638 24. **Gawarzewski I, Smits SH, Schmitt L, Jose J.** 2013. Structural comparison of the
639 transport units of type V secretion systems. *Biol Chem* **394**:1385-1398.
- 640 25. **Grijpstra J, Arenas J, Rutten L, Tommassen J.** 2013. Autotransporter secretion:
641 varying on a theme. *Res Microbiol* **164**:562-582.
- 642 26. **Benz I, Schmidt MA.** 2011. Structures and functions of autotransporter proteins in
643 microbial pathogens. *Int J Med Microbiol* **301**:461-468.
- 644 27. **Ieva R, Bernstein HD.** 2009. Interaction of an autotransporter passenger domain with
645 BamA during its translocation across the bacterial outer membrane. *Proc Natl Acad Sci U*
646 *S A* **106**:19120-19125.
- 647 28. **Sauri A, Soprova Z, Wickstrom D, de Gier JW, Van der Schors RC, Smit AB, Jong**
648 **WS, Luirink J.** 2009. The Bam (Omp85) complex is involved in secretion of the
649 autotransporter haemoglobin protease. *Microbiology* **155**:3982-3991.
- 650 29. **Selkrig J, Mosbahi K, Webb CT, Belousoff MJ, Perry AJ, Wells TJ, Morris F,**
651 **Leyton DL, Totsika M, Phan MD, Celik N, Kelly M, Oates C, Hartland EL, Robins-**
652 **Browne RM, Ramarathinam SH, Purcell AW, Schembri MA, Strugnell RA,**
653 **Henderson IR, Walker D, Lithgow T.** 2012. Discovery of an archetypal protein
654 transport system in bacterial outer membranes. *Nat Struct Mol Biol* **19**:506-510, S501.
- 655 30. **Jain S, Goldberg MB.** 2007. Requirement for YaeT in the outer membrane assembly of
656 autotransporter proteins. *J Bacteriol* **189**:5393-5398.

- 657 31. **Henderson IR, Navarro-Garcia F, Desvaux M, Fernandez RC, Ala'Aldeen D.** 2004.
658 Type V protein secretion pathway: the autotransporter story. *Microbiol Mol Biol Rev*
659 **68**:692-744.
- 660 32. **Desvaux M, Parham NJ, Henderson IR.** 2004. Type V protein secretion: simplicity
661 gone awry? *Curr Issues Mol Biol* **6**:111-124.
- 662 33. **Nishimura K, Tajima N, Yoon YH, Park SY, Tame JR.** 2010. Autotransporter
663 passenger proteins: virulence factors with common structural themes. *J Mol Med (Berl)*
664 **88**:451-458.
- 665 34. **Yen YT, Kostakioti M, Henderson IR, Stathopoulos C.** 2008. Common themes and
666 variations in serine protease autotransporters. *Trends Microbiol* **16**:370-379.
- 667 35. **Dautin N.** 2010. Serine protease autotransporters of *Enterobacteriaceae* (SPATEs):
668 biogenesis and function. *Toxins (Basel)* **2**:1179-1206.
- 669 36. **Ruiz-Perez F, Nataro JP.** 2014. Bacterial serine proteases secreted by the
670 autotransporter pathway: classification, specificity, and role in virulence. *Cell Mol Life*
671 *Sci* **71**:745-770.
- 672 37. **Dutta PR, Cappello R, Navarro-Garcia F, Nataro JP.** 2002. Functional comparison of
673 serine protease autotransporters of *Enterobacteriaceae*. *Infect Immun* **70**:7105-7113.
- 674 38. **Djafari S, Ebel F, Deibel C, Kramer S, Hudel M, Chakraborty T.** 1997.
675 Characterization of an exported protease from Shiga toxin-producing *Escherichia coli*.
676 *Mol Microbiol* **25**:771-784.
- 677 39. **Stein M, Kenny B, Stein MA, Finlay BB.** 1996. Characterization of EspC, a 110-
678 kilodalton protein secreted by enteropathogenic *Escherichia coli* which is homologous to
679 members of the immunoglobulin A protease-like family of secreted proteins. *J Bacteriol*
680 **178**:6546-6554.
- 681 40. **Guyer DM, Henderson IR, Nataro JP, Mobley HL.** 2000. Identification of Sat, an
682 autotransporter toxin produced by uropathogenic *Escherichia coli*. *Mol Microbiol* **38**:53-
683 66.
- 684 41. **Al-Hasani K, Henderson IR, Sakellaris H, Rajakumar K, Grant T, Nataro JP,**
685 **Robins-Browne R, Adler B.** 2000. The *sigA* gene which is borne on the *she*
686 pathogenicity island of *Shigella flexneri 2a* encodes an exported cytopathic protease
687 involved in intestinal fluid accumulation. *Infect Immun* **68**:2457-2463.
- 688 42. **Navarro-Garcia F, Canizalez-Roman A, Sui BQ, Nataro JP, Azamar Y.** 2004. The
689 serine protease motif of EspC from enteropathogenic *Escherichia coli* produces epithelial
690 damage by a mechanism different from that of pet toxin from enteroaggregative *E. coli*.
691 *Infect Immun* **72**:3609-3621.
- 692 43. **Henderson IR, Hicks S, Navarro-Garcia F, Elias WP, Philips AD, Nataro JP.** 1999.
693 Involvement of the enteroaggregative *Escherichia coli* plasmid-encoded toxin in causing
694 human intestinal damage. *Infect Immun* **67**:5338-5344.
- 695 44. **Ruiz-Perez F, Wahid R, Faherty CS, Kolappaswamy K, Rodriguez L, Santiago A,**
696 **Murphy E, Cross A, Sztein MB, Nataro JP.** 2011. Serine protease autotransporters
697 from *Shigella flexneri* and pathogenic *Escherichia coli* target a broad range of leukocyte
698 glycoproteins. *Proc Natl Acad Sci U S A* **108**:12881-12886.
- 699 45. **Parham NJ, Pollard SJ, Desvaux M, Scott-Tucker A, Liu C, Fivian A, Henderson**
700 **IR.** 2005. Distribution of the serine protease autotransporters of the *Enterobacteriaceae*
701 among extraintestinal clinical isolates of *Escherichia coli*. *J Clin Microbiol* **43**:4076-
702 4082.

- 703 46. **Parreira VR, Gyles CL.** 2003. A novel pathogenicity island integrated adjacent to the
704 *thrW* tRNA gene of avian pathogenic *Escherichia coli* encodes a vacuolating
705 autotransporter toxin. *Infect Immun* **71**:5087-5096.
- 706 47. **Simms AN, Mobley HL.** 2008. PapX, a P fimbrial operon-encoded inhibitor of motility
707 in uropathogenic *Escherichia coli*. *Infect Immun* **76**:4833-4841.
- 708 48. **Reiss DJ, Mobley HL.** 2011. Determination of target sequence bound by PapX,
709 repressor of bacterial motility, in *flhD* promoter using systematic evolution of ligands by
710 exponential enrichment (SELEX) and high throughput sequencing. *J Biol Chem*
711 **286**:44726-44738.
- 712 49. **Simms AN, Mobley HL.** 2008. Multiple genes repress motility in uropathogenic
713 *Escherichia coli* constitutively expressing type 1 fimbriae. *J Bacteriol* **190**:3747-3756.
- 714 50. **Subashchandrabose S, Smith SN, Spurbeck RR, Kole MM, Mobley HLT.** 2013.
715 Genome-Wide Detection of Fitness Genes in Uropathogenic *Escherichia coli* during
716 Systemic Infection. *PLoS Pathog* **9**.
- 717 51. **Otto BR, van Dooren SJ, Nuijens JH, Luirink J, Oudega B.** 1998. Characterization of
718 a hemoglobin protease secreted by the pathogenic *Escherichia coli* strain EB1. *J Exp*
719 *Med* **188**:1091-1103.
- 720 52. **Provence DL, Curtiss R, 3rd.** 1994. Isolation and characterization of a gene involved in
721 hemagglutination by an avian pathogenic *Escherichia coli* strain. *Infect Immun* **62**:1369-
722 1380.
- 723 53. **Otto BR, Sijbrandi R, Luirink J, Oudega B, Heddle JG, Mizutani K, Park SY,
724 Tame JR.** 2005. Crystal structure of hemoglobin protease, a heme binding
725 autotransporter protein from pathogenic *Escherichia coli*. *J Biol Chem* **280**:17339-17345.
- 726 54. **Tame JRH, van Dooren SJM, Oudega B, Otto BR.** 2002. Characterization and
727 crystallization of a novel haemoglobinase from pathogenic *Escherichia coli*. *Acta*
728 *Crystallogr D Biol Crystallogr* **58**:843-845.
- 729 55. **Nishimura K, Yoon YH, Kurihara A, Unzai S, Luirink J, Park SY, Tame JRH.**
730 2010. Role of domains within the autotransporter Hbp/Tsh. *Acta Crystallogr D Biol*
731 *Crystallogr* **66**:1295-1300.
- 732 56. **van Dooren SJM, Tame JRH, Luirink J, Oudega B, Otto BR.** 2001. Purification of
733 the autotransporter protein Hbp of *Escherichia coli*. *Fems Microbiol Lett* **205**:147-150.
- 734 57. **Kobayashi RK, Gaziri LC, Vidotto MC.** 2010. Functional activities of the Tsh protein
735 from avian pathogenic *Escherichia coli* (APEC) strains. *J Vet Sci* **11**:315-319.
- 736 58. **Welch RA, Burland V, Plunkett G, 3rd, Redford P, Roesch P, Rasko D, Buckles EL,
737 Liou SR, Boutin A, Hackett J, Stroud D, Mayhew GF, Rose DJ, Zhou S, Schwartz
738 DC, Perna NT, Mobley HL, Sonnenberg MS, Blattner FR.** 2002. Extensive mosaic
739 structure revealed by the complete genome sequence of uropathogenic *Escherichia coli*.
740 *Proc Natl Acad Sci U S A* **99**:17020-17024.
- 741 59. **Heimer SR, Rasko DA, Lockett CV, Johnson DE, Mobley HLT.** 2004.
742 Autotransporter genes *pic* and *tsh* are associated with *Escherichia coli* strains that cause
743 acute pyelonephritis and are expressed during urinary tract infection. *Infect Immun*
744 **72**:593-597.
- 745 60. **Mobley HLT, Green DM, Trifillis AL, Johnson DE, Chippendale GR, Lockett CV,
746 Jones BD, Warren JW.** 1990. Pyelonephritogenic *Escherichia coli* and Killing of
747 Cultured Human Renal Proximal Tubular Epithelial Cells: Role of Hemolysin in Some
748 Strains. *Infect Immun* **58**:1281-1289.

- 749 61. **Moriel DG, Bertoldi I, Spagnuolo A, Marchi S, Rosini R, Nesta B, Pastorello I,**
750 **Corea VA, Torricelli G, Cartocci E, Savino S, Scarselli M, Dobrindt U, Hacker J,**
751 **Tettelin H, Tallon LJ, Sullivan S, Wieler LH, Ewers C, Pickard D, Dougan G,**
752 **Fontana MR, Rappuoli R, Pizza M, Serino L.** 2010. Identification of protective and
753 broadly conserved vaccine antigens from the genome of extraintestinal pathogenic
754 *Escherichia coli*. *Proc Natl Acad Sci U S A* **107**:9072-9077.
- 755 62. **LeClerc JE, Li BG, Payne WL, Cebula TA.** 1996. High mutation frequencies among
756 *Escherichia coli* and *Salmonella* pathogens. *Science* **274**:1208-1211.
- 757 63. **Blattner FR, Plunkett G, 3rd, Bloch CA, Perna NT, Burland V, Riley M, Collado-**
758 **Vides J, Glasner JD, Rode CK, Mayhew GF, Gregor J, Davis NW, Kirkpatrick HA,**
759 **Goeden MA, Rose DJ, Mau B, Shao Y.** 1997. The complete genome sequence of
760 *Escherichia coli* K-12. *Science* **277**:1453-1462.
- 761 64. **Jeong H, Barbe V, Lee CH, Vallenet D, Yu DS, Choi SH, Couloux A, Lee SW, Yoon**
762 **SH, Cattolico L, Hur CG, Park HS, Segurens B, Kim SC, Oh TK, Lenski RE,**
763 **Studier FW, Daegelen P, Kim JF.** 2009. Genome sequences of *Escherichia coli* B
764 strains REL606 and BL21(DE3). *J Mol Biol* **394**:644-652.
- 765 65. **Ochman H, Selander RK.** 1984. Standard reference strains of *Escherichia coli* from
766 natural populations. *J Bacteriol* **157**:690-693.
- 767 66. **Rutherford K, Parkhill J, Crook J, Horsnell T, Rice P, Rajandream MA, Barrell B.**
768 2000. Artemis: sequence visualization and annotation. *Bioinformatics* **16**:944-945.
- 769 67. **Sullivan MJ, Petty NK, Beatson SA.** 2011. Easyfig: a genome comparison visualizer.
770 *Bioinformatics* **27**:1009-1010.
- 771 68. **Sievers F, Wilm A, Dineen D, Gibson TJ, Karplus K, Li W, Lopez R, McWilliam H,**
772 **Remmert M, Soding J, Thompson JD, Higgins DG.** 2011. Fast, scalable generation of
773 high-quality protein multiple sequence alignments using Clustal Omega. *Mol Syst Biol*
774 **7**:539.
- 775 69. **Goujon M, McWilliam H, Li W, Valentin F, Squizzato S, Paern J, Lopez R.** 2010. A
776 new bioinformatics analysis tools framework at EMBL-EBI. *Nucleic Acids Res*
777 **38**:W695-699.
- 778 70. **Rambaut A, Drummond A.** 2009. FigTree, v1.4.2.
779 <http://tree.bio.ed.ac.uk/software/figtree/>.
- 780 71. **Sambrook J, Fritsch, E. F. & Maniatis, T.** 2001. Molecular cloning: a laboratory
781 manual, 3rd ed. Cold Spring Harbor Laboratory Press, New York.
- 782 72. **Wirth T, Falush D, Lan R, Colles F, Mensa P, Wieler LH, Karch H, Reeves PR,**
783 **Maiden MC, Ochman H, Achtman M.** 2006. Sex and virulence in *Escherichia coli*: an
784 evolutionary perspective. *Mol Microbiol* **60**:1136-1151.
- 785 73. **Datsenko KA, Wanner BL.** 2000. One-step inactivation of chromosomal genes in
786 *Escherichia coli* K-12 using PCR products. *Proc Natl Acad Sci U S A* **97**:6640-6645.
- 787 74. **Martinez E, Bartolome B, de la Cruz F.** 1988. pACYC184-derived cloning vectors
788 containing the multiple cloning site and *lacZa* reporter gene of pUC8/9 and pUC18/19
789 plasmids. *Gene* **68**:159-162.
- 790 75. **Livak KJ, Schmittgen TD.** 2001. Analysis of relative gene expression data using real-
791 time quantitative PCR and the $2^{-\Delta\Delta CT}$ method. *Methods* **25**:402-408.
- 792 76. **Munch R, Hiller K, Grote A, Scheer M, Klein J, Schobert M, Jahn D.** 2005. Virtual
793 Footprint and PRODORIC: an integrative framework for regulon prediction in
794 prokaryotes. *Bioinformatics* **21**:4187-4189.

- 795 77. **Beloin C, Dorman CJ.** 2003. An extended role for the nucleoid structuring protein H-NS
796 in the virulence gene regulatory cascade of *Shigella flexneri*. *Mol Microbiol* **47**:825-838.
- 797 78. **Ulett GC, Webb RI, Schembri MA.** 2006. Antigen-43-mediated autoaggregation
798 impairs motility in *Escherichia coli*. *Microbiology* **152**:2101-2110.
- 799 79. **Delcastillo I, Gomez JM, Moreno F.** 1990. *mprA*, an *Escherichia coli* Gene That
800 Reduces Growth-Phase-Dependent Synthesis of Microcin-B17 and Microcin-C7 and
801 Blocks Osmoinduction of *proU* When Cloned on a High-Copy-Number Plasmid. *J*
802 *Bacteriol* **172**:437-445.
- 803 80. **Sjostrom AE, Sonden B, Muller C, Rydstrom A, Dobrindt U, Wai SN, Uhlin BE.**
804 2009. Analysis of the *sfaX(II)* locus in the *Escherichia coli* meningitis isolate IHE3034
805 reveals two novel regulatory genes within the promoter-distal region of the main S
806 fimbrial operon. *Microb Pathog* **46**:150-158.
- 807 81. **Lomovskaya O, Lewis K, Matin A.** 1995. Emrr Is a Negative Regulator of the
808 *Escherichia coli* Multidrug Resistance Pump EmrAB. *J Bacteriol* **177**:2328-2334.
- 809 82. **Roper DI, Fawcett T, Cooper RA.** 1993. The *Escherichia coli* C Homoprotocatechuate
810 Degradative Operon: *hpc* Gene Order, Direction of Transcription and Control of
811 Expression. *Mol Gen Genet* **237**:241-250.
- 812 83. **Paracuellos P, Ohman A, Sauer-Eriksson AE, Uhlin BE.** 2012. Expression and
813 purification of SfaX(II), a protein involved in regulating adhesion and motility genes in
814 extraintestinal pathogenic *Escherichia coli*. *Protein Expr Purif* **86**:127-134.
- 815 84. **Dezfulian H, Tremblay D, Harel J.** 2004. Molecular characterization of extraintestinal
816 pathogenic *Escherichia coli* (ExPEC) pathogenicity islands in F165-positive *E. coli* strain
817 from a diseased animal. *FEMS Microbiol Lett* **238**:321-332.
- 818 85. **Lang B, Blot N, Bouffartigues E, Buckle M, Geertz M, Gualerzi CO, Mavathur R,**
819 **Muskhelishvili G, Pon CL, Rimsky S, Stella S, Babu MM, Travers A.** 2007. High-
820 affinity DNA binding sites for H-NS provide a molecular basis for selective silencing
821 within proteobacterial genomes. *Nucleic Acids Research* **35**:6330-6337.
- 822 86. **Yang J, Tauschek M, Strugnell R, Robins-Browne RM.** 2005. The H-NS protein
823 represses transcription of the *eltAB* operon, which encodes heat-labile enterotoxin in
824 enterotoxigenic *Escherichia coli*, by binding to regions downstream of the promoter.
825 *Microbiology-Sgm* **151**:1199-1208.
- 826 87. **Scott ME, Melton-Celsa AR, O'Brien AD.** 2003. Mutations in *hms* reduce the adherence
827 of Shiga toxin-producing *E. coli* 091 : H21 strain B2F1 to human colonic epithelial cells
828 and increase the production of hemolysin. *Microb Pathog* **34**:155-159.
- 829 88. **Lithgow JK, Haider F, Roberts IS, Green J.** 2007. Alternate SlyA and H-NS
830 nucleoprotein complexes control *hlyE* expression in *Escherichia coli* K-12. *Mol*
831 *Microbiol* **66**:685-698.
- 832 89. **Li HP, Granat A, Stewart V, Gillespie JR.** 2008. RpoS, H-NS, and DsrA influence
833 EHEC hemolysin operon (*ehxCABD*) transcription in *Escherichia coli* O157 : H7 strain
834 EDL933. *FEMS Microbiol Lett* **285**:257-262.
- 835 90. **Allsopp LP, Beloin C, Moriel DG, Totsika M, Ghigo JM, Schembri MA.** 2012.
836 Functional heterogeneity of the UpaH autotransporter protein from uropathogenic
837 *Escherichia coli*. *J Bacteriol* **194**:5769-5782.
- 838 91. **Bolivar F, Rodriguez RL, Greene PJ, Betlach MC, Heyneker HL, Boyer HW, Crosa**
839 **JH, Falkow S.** 1977. Construction and characterization of new cloning vehicle. II. A
840 multipurpose cloning system. *Gene* **2**:95-113.

- 841 92. **Ko M, Park C.** 2000. Two novel flagellar components and H-NS are involved in the
842 motor function of *Escherichia coli*. *J Mol Biol* **303**:371-382.
- 843 93. **McVicker G, Sun L, Sohanpal BK, Gashi K, Williamson RA, Plumbridge J,**
844 **Blomfield IC.** 2011. SlyA Protein Activates *fimB* Gene Expression and Type 1
845 Fimbriation in *Escherichia coli* K-12. *Journal of Biological Chemistry* **286**:32026-32035.
- 846 94. **Nielubowicz GR, Mobley HL.** 2010. Host-pathogen interactions in urinary tract
847 infection. *Nat Rev Urol* **7**:430-441.
- 848 95. **Totsika M, Moriel DG, Idris A, Rogers BA, Wурpel DJ, Phan MD, Paterson DL,**
849 **Schembri MA.** 2012. Uropathogenic *Escherichia coli* mediated urinary tract infection.
850 *Curr Drug Targets* **13**:1386-1399.
- 851 96. **Spurbeck RR, Dinh PC, Walk ST, Stapleton AE, Hooton TM, Nolan LK, Kim KS,**
852 **Johnson JR, Mobley HLT.** 2012. *Escherichia coli* Isolates That Carry *vat*, *fyuA*, *chuA*,
853 and *yfcV* Efficiently Colonize the Urinary Tract. *Infect Immun* **80**:4115-4122.
- 854 97. **Dorman CJ.** 2007. H-NS, the genome sentinel. *Nat Rev Microbiol* **5**:157-161.
- 855 98. **Goransson M, Sonden B, Nilsson P, Dagberg B, Forsman K, Emanuelsson K, Uhlin**
856 **BE.** 1990. Transcriptional silencing and thermoregulation of gene expression in
857 *Escherichia coli*. *Nature* **344**:682-685.
- 858 99. **Atlung T, Ingmer H.** 1997. H-NS: a modulator of environmentally regulated gene
859 expression. *Mol Microbiol* **24**:7-17.
- 860 100. **Amit R, Oppenheim AB, Stavans J.** 2003. Increased bending rigidity of single DNA
861 molecules by H-NS, a temperature and osmolarity sensor. *Biophys J* **84**:2467-2473.
- 862 101. **Lucchini S, Rowley G, Goldberg MD, Hurd D, Harrison M, Hinton JC.** 2006. H-NS
863 mediates the silencing of laterally acquired genes in bacteria. *PLoS Pathog* **2**:e81.
- 864 102. **Wilkinson SP, Grove A.** 2006. Ligand-responsive transcriptional regulation by members
865 of the MarR family of winged helix proteins. *Curr Issues Mol Biol* **8**:51-62.
- 866 103. **Ellison DW, Miller VL.** 2006. Regulation of virulence by members of the MarR/SlyA
867 family. *Curr Opin Microbiol* **9**:153-159.
- 868

869 **FIGURE LEGENDS**

870

871 **FIG. 1.** (A) BLAST alignment demonstrating the level of nucleotide sequence conservation
872 (grey shading) for *vat* and *vatX* (labelled red), as well as the other surrounding genes (labelled
873 blue). The Vat-PAI (defined by the *proA* and *yagU* genes [labelled yellow]) was identified in 14
874 of 77 complete *E. coli* genomes examined. These sequences were compared to the Vat-PAI
875 originally identified in the avian pathogenic *E. coli* strain Ec222 (top). (B) Immunodetection of
876 the Vat passenger domain (Vat α) from supernatant fractions prepared from overnight cultures of
877 the well-characterised UPEC strains CFT073, IHE3034 and 536. Vat expression by MG1655
878 (pVat) is shown as a positive control, while MG1655(pSU2718) and CFT073*vat* were included
879 as a negative controls.

880

881 **FIG. 2.** Phylogram demonstrating the relationship between representative *E. coli* MarR-type
882 regulator proteins. The scale represents the number of amino acid substitutions per site over 194
883 positions.

884

885 **FIG. 3.** (A) qRT-PCR analysis of *vat* transcription in CFT073*vatX* and CFT073*vatX*(pVatX)
886 compared to wild-type CFT073. The transcription of *vat* was significantly increased in
887 CFT073*vatX*(pVatX) compared to CFT073 (** $P < 0.01$). (B) Western blot analysing the effect of
888 VatX on Vat expression. Supernatant fractions were prepared from overnight cultures of
889 MG1655(pVat), MG1655(pSU2718), CFT073(pSU2718), CFT073(pVatX),
890 CFT073*vatX*(pSU2718) and CFT073*vatX*(pVatX). Over-expression of VatX led to an increase in
891 the amount Vat detected in the culture supernatant.

892

893 **FIG. 4.** (A) Schematic of the *vat-vatX* gene operon in CFT073. The position of the promoter and
894 primers used to identify *vat-vatX* and *vatX* transcripts is indicated. The inset shows the *vat* gene
895 transcriptional start site (+1), which was mapped to 80bp upstream of the ATG start codon (grey
896 arrow). Also indicated are the consensus -10 and -35 promoter elements and the three putative H-
897 NS nucleation sites (shown in bold). (B) Immunodetection of the Vat passenger domain from the
898 supernatant fractions of CFT073, CFT073*vat*, CFT073*vatX*, CFT073*hns* and CFT073*vatX hns*.
899 The level of Vat was increased in CFT073*hns* and CFT073*vatX hns* compared to CFT073. (C)
900 EMSA demonstrating the direct interaction of H-NS with the *vat* promoter region. The assay was
901 performed using a 252bp fragment encompassing the *vat* promoter region (indicated by an
902 asterisk), a 218bp fragment containing the *bla* promoter region amplified from pBR322 (positive
903 control: indicated by an arrow), and three additional DNA fragments amplified from pBR322
904 (negative controls: 152bp, 312bp and 479bp). Native H-NS protein was incubated with the DNA
905 in increasing concentrations (0 μ M H-NS, 0.1 μ M H-NS, 0.5 μ M H-NS and 1.0 μ M H-NS). (D)
906 Transcriptional analysis of the *vat* and *vatX* genes. Total RNA was extracted during exponential
907 growth of CFT073*hns* and converted to cDNA. Shown are the PCR products [*vat-vatX* (1112bp)
908 or *vatX* (404bp)] amplified from CFT073*hns* gDNA (positive control), total RNA (negative
909 control) and cDNA.

910

911 **FIG. 5.** (A) Diagram depicting the full length Vat primary protein sequence, including three
912 protein domains typical for SPATES: i) the extended signal peptide (SP); ii) the passenger
913 domain comprising the Immunoglobulin A1 protease-like domain, which contains the serine
914 protease motif, as well as the upstream aspartate (D158) and histidine (H130) residues of the
915 catalytic triad; and iii) the translocation domain, which is cleaved at the alpha-helical linker
916 region. Class II SPATEs are characterised by the presence of a small additional domain termed
917 Domain 2 (striped). Two variable regions (VR1 and VR2) located within the passenger domain
918 were identified (triangles). (B) Alignment of the Vat amino acid sequence in VR1 and VR2 from
919 CFT073 and the ten strains representing the diverse STs examined. Residues identical to those in
920 Vat from CFT073 are indicated by dots; residues that differed from the CFT073 sequence are
921 indicated and highlighted in grey. Vat secretion was determined by Western blot analysis of the
922 supernatant fractions from each strain following overnight growth in LB broth at 37°C. All
923 strains secreted a ~110kDa protein that cross-reacted with the Vat-specific polyclonal antibody
924 (indicated as +).

925

926 **FIG. 6.** Immunoreactivity of Vat. Blood plasma was collected from 45 urosepsis patients at the
927 time of admittance to hospital. Paired UPEC strains were also isolated from the blood of each
928 patient, and the presence of the *vat* gene was determined by PCR. Plasma samples were
929 subsequently grouped by their association with *vat*-positive (Vat+) or *vat*-negative (Vat-) strains.
930 The presence of IgG-specific antibodies was determined by ELISA, and compared to results
931 obtained from 42 healthy volunteers with no recent history of UTI (Healthy). A significantly
932 higher IgG titre was observed in plasma of patients infected with Vat+ strains compared to
933 patients infected with Vat- strains and healthy controls.

934

935

936 **Supplementary Information**

937

938 **Figure S1.** Cladogram demonstrating the relationship of the 330 MarR-type regulator protein
939 sequences identified in the 77 complete *E. coli* genomes listed in Table S1. The scale represents
940 the number of amino acid substitutions per site over 194 positions.

941

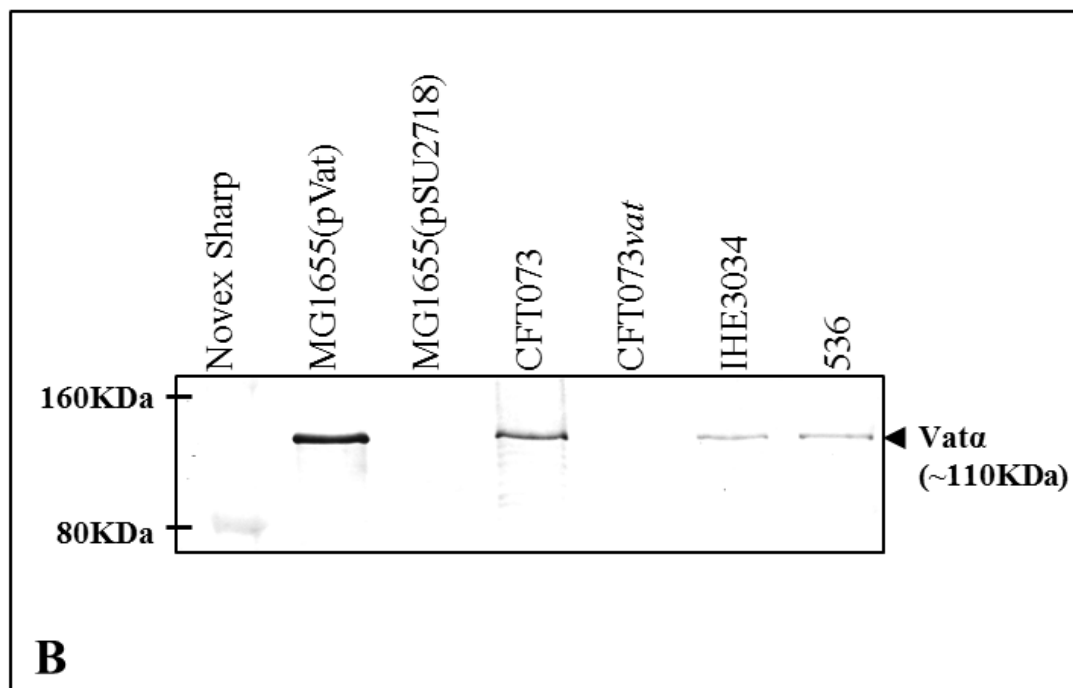
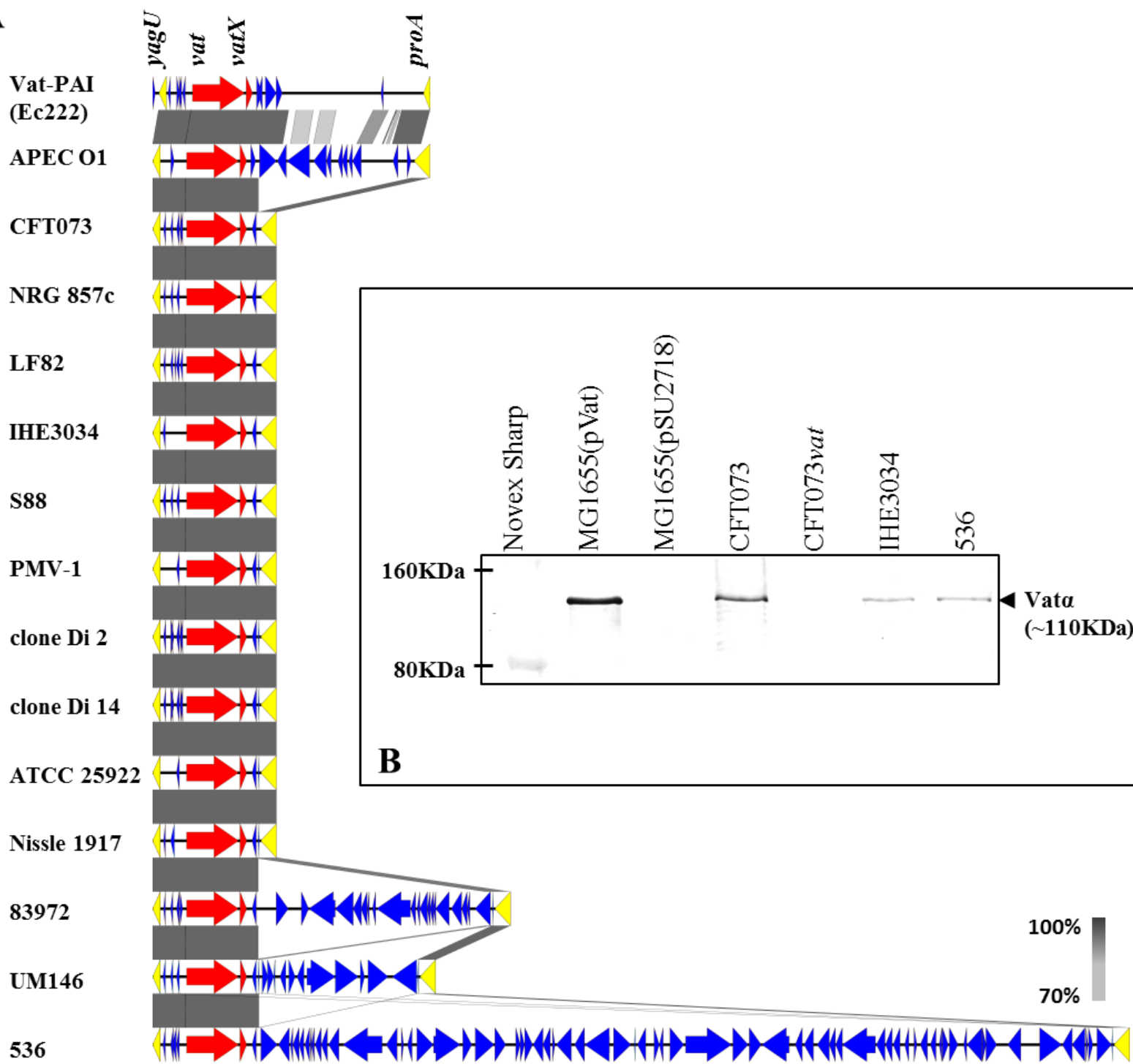
942 **Figure S2.** Vat catalytic triad and VIR1/2 regions mapped using the crystal structure of
943 hemoglobin protease (Hbp) passenger domain (3AK5). Hbp is the most related SPATE to Vat,
944 sharing 79% amino acid identity. The structural protein mapping indicates that VIR1/2 are not
945 directly associated with the globular catalytic triad.

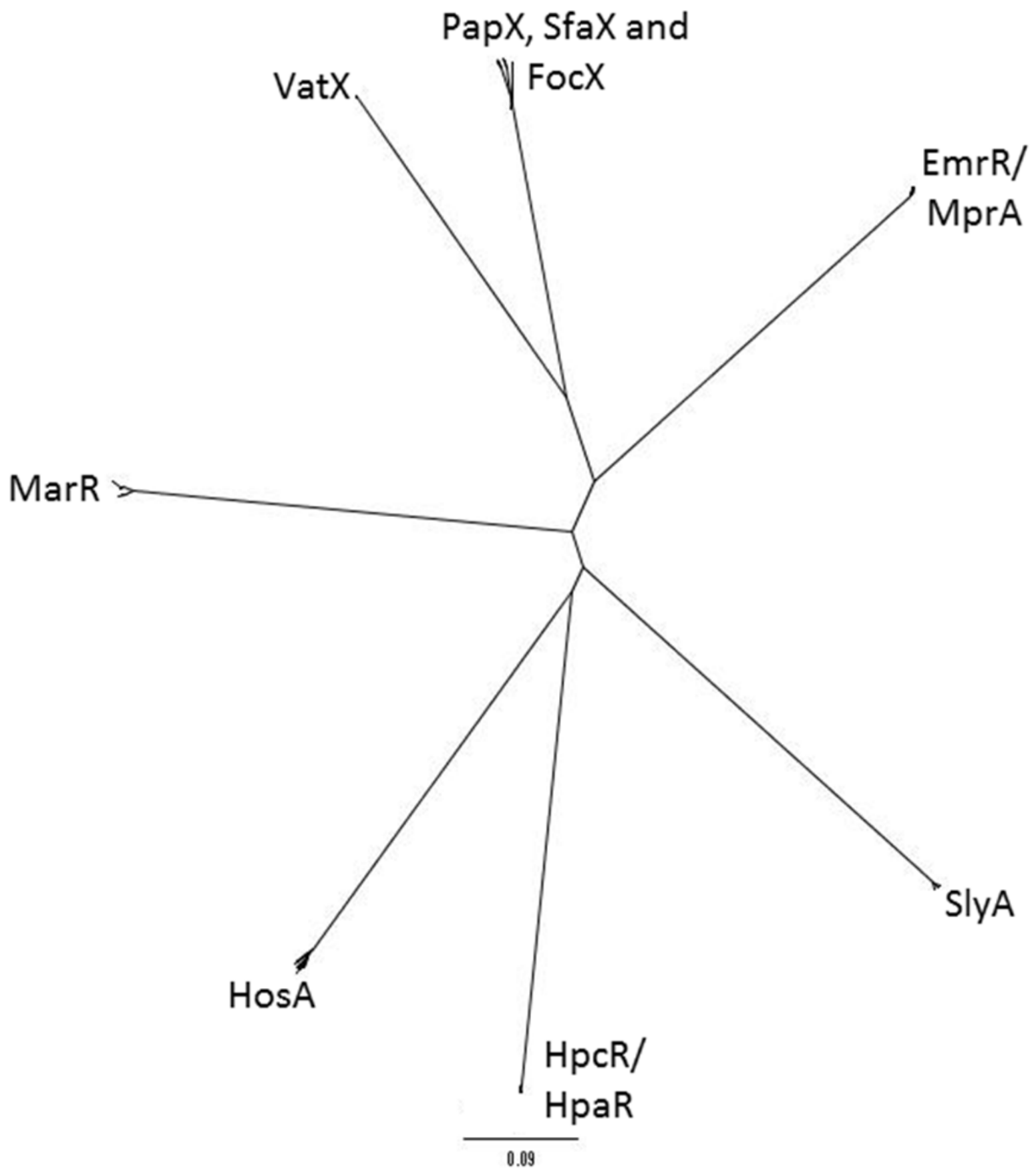
946

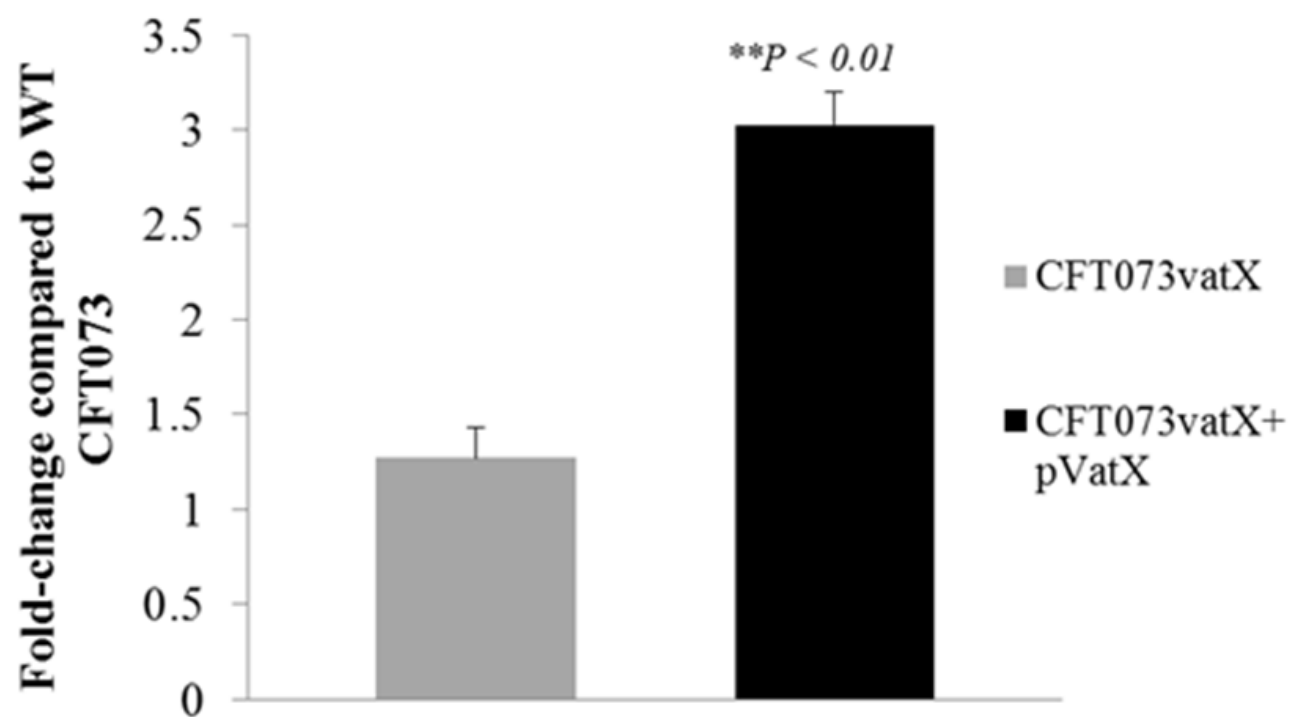
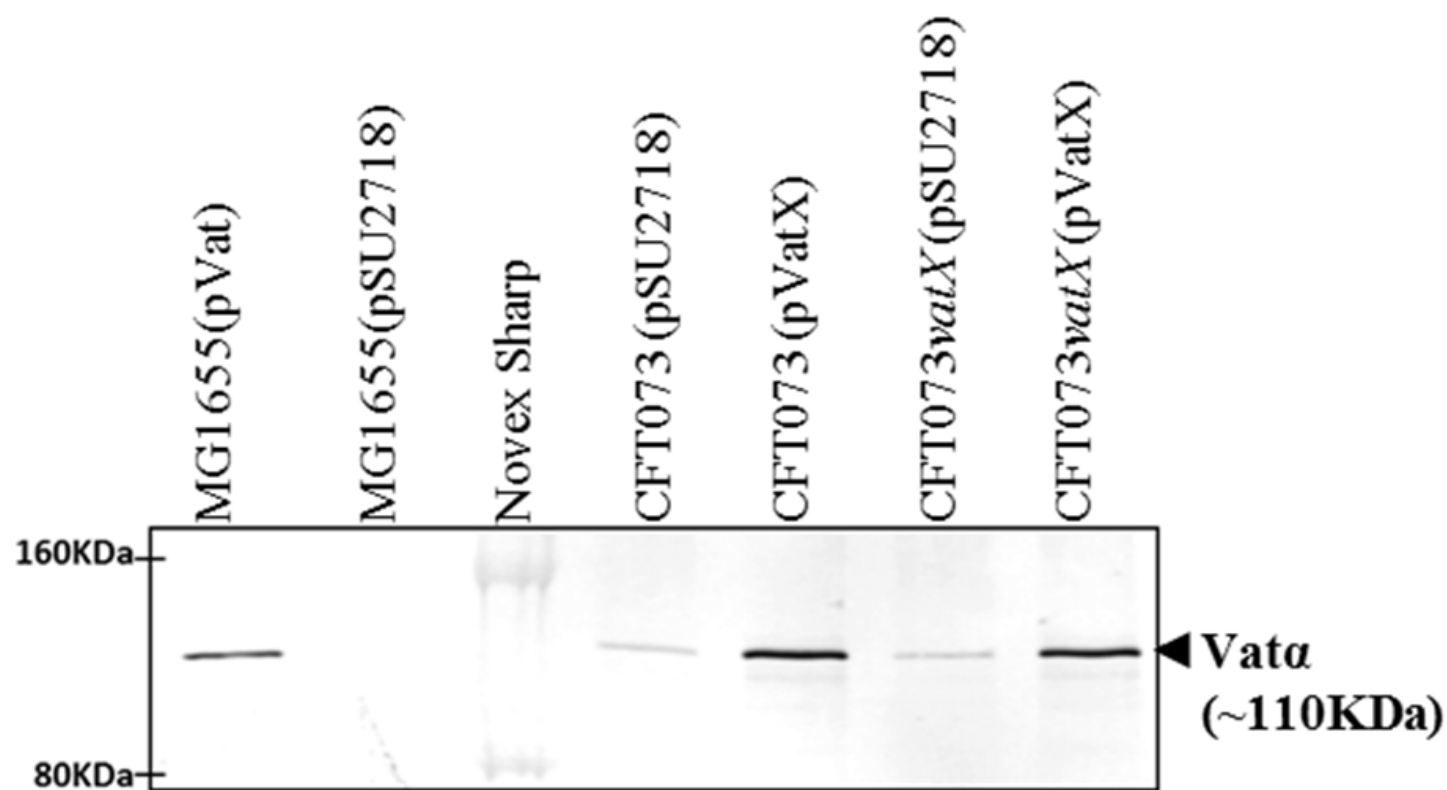
947 **Table S1.** List of the 77 sequenced *E. coli* genomes obtained from the NCBI website. The strains
948 include a selection of environmental, non-pathogenic (NP) and pathogenic *E. coli*. The list
949 includes the following *E. coli* pathotypes: enteropathogenic *E. coli* (EPEC), enterotoxigenic *E.*
950 *coli* (ETEC), adherent-invasive *E. coli* (AIEC), enterohaemorrhagic *E. coli* (EHEC),
951 enteroaggregative haemorrhagic *E. coli* (EAHEC), Shiga toxin-producing *E. coli* (STEC),
952 neonatal meningitis *E. coli* (NMEC), uropathogenic *E. coli* (UPEC) and avian pathogenic *E. coli*
953 (APEC).

954

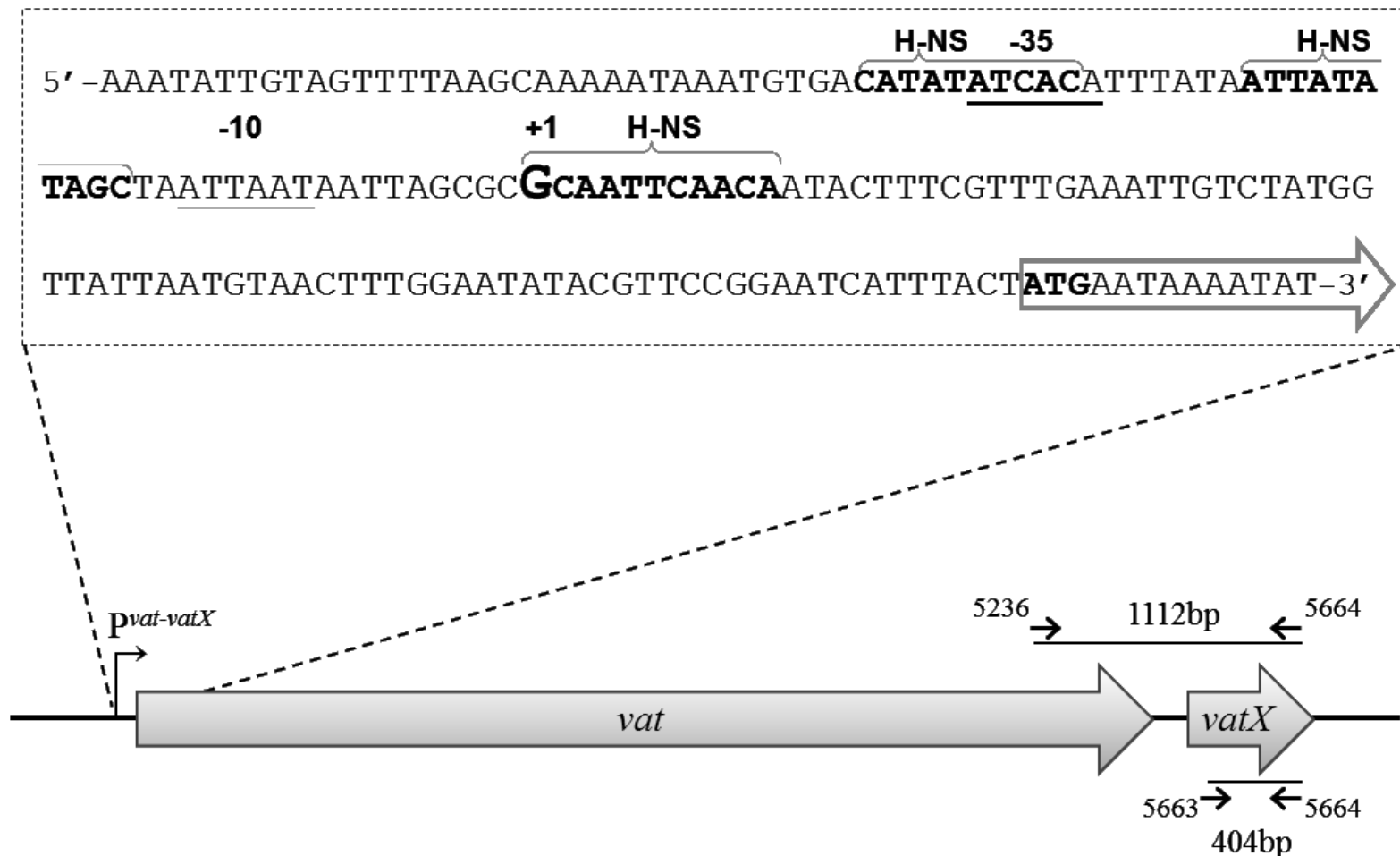
955 **Table S2.** MarR-type transcriptional regulator genes identified in the 77 complete *E. coli*
956 genomes described in Table S1. The representative genes used as query sequences in the BLAST
957 analysis are underlined. These sequences were used to generate the phylogram in Figure 2. Seven
958 major clades were identified, MarR; MprA/EmrR; HosA; HpcR/HpaR; SlyA; SfaX/FocX/PapX
959 and VatX. The level of amino acid sequence identity for proteins in each clade is indicated.

A**B**

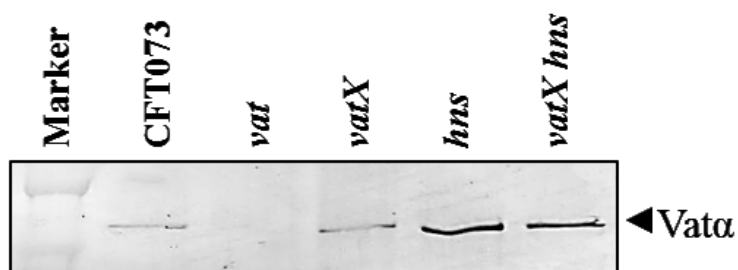


A**B**

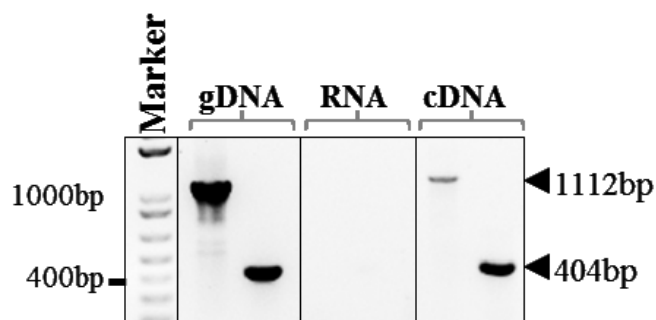
A



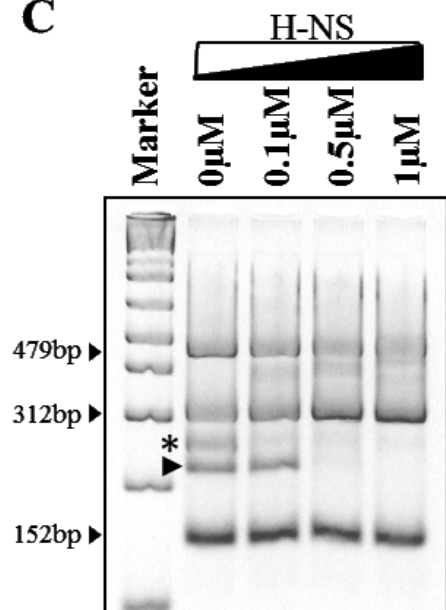
B

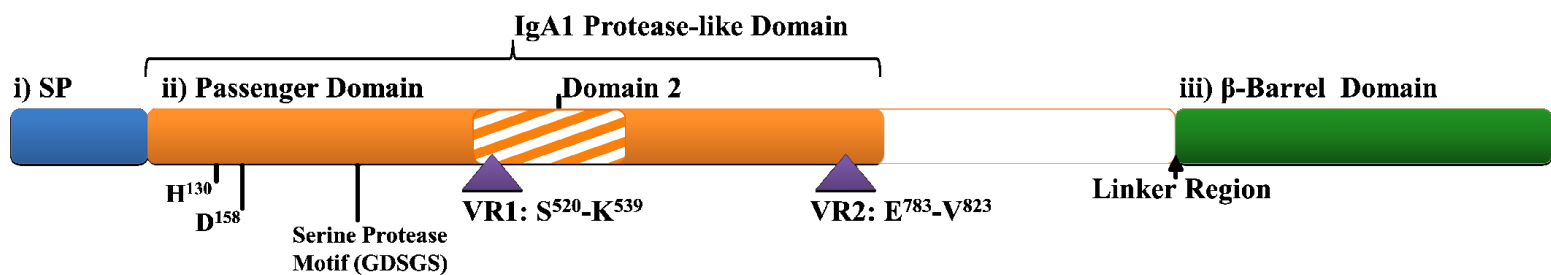


D



C





A

Strain	VR1	VR2	ST	Vat
CFT073	SSDKTANILTLDYQTRPADVK	EIFNGGIQANNSTVNISSDSAVLENSTLTSTALNLNKGANV	ST 73	+
PA48B	ST 73	+
PA10BN..	ST 95	+
PA38B	D.....I.G.....A	ST 537	+
PA32BH.....	D...I.....I.G.....A	ST Unknown	+
PA60BH.....	D.....I.G.....A	ST Unknown	+
PA15BH.....	D.....I.G.....A	ST 12	+
PA56BH.....	D.....I.G.....A	ST 2800	+
PA42BH.....	ST 420	+

B

Absorbance at 450nm

